Significance of NRROS in CNS Homeostasis

Amr Makhamreh

Biomolecular Engineering

April 3, 2019

Abstract

Negative regulator for reactive oxygen species, also known as NRROS, is a protein that is highly expressed in the endoplasmic reticulum of immune cells with phagocytic capabilities. NRROS is responsible for regulating the production of reactive oxygen species (ROS) during inflammatory responses. The role of NRROS is crucial in preventing collateral tissue damage because ROS are highly reactive chemical species that adversely alter all macromolecules, hence being toxic for your cells. Recent studies have shown that the deletion of NRROS in mice leads to spontaneous neurological disorders and ultimately early mortality at 6 months of age.

The goal of this research project was to observe and describe the neurological defects associated with the absence of NRROS in the central nervous system (CNS) of mice, with the aim of figuring out what defect causes early mortality in these mice. The implementation of the cre-lox recombinase system allowed for NRROS to be partially expressed (heterozygous) or fully absent (mutant) in the CNS myeloid cells of mice. To analyze the deleterious effects of an NRROS-deficient environment on the CNS, I extracted and sectioned the brains of heterozygous mice and mutant mice, conducted immunohistochemistry stainings that targeted specific neuroglia cells, and conducted a comparative analysis between the heterozygous and mutant brains. Results confirmed the presence of astrogliosis, a hallmark of neurodegenerative diseases. Also, data from the mutant antibody stainings displayed that there is a complete loss of steady state and activated microglia cells, which are the brain tissue-resident immune cell, and instead an emergence of an activated immune cell described as PLC macrophages. The loss of microglia

and the presence of PLCs indicates that NRROS plays a cell-intrinsic role in microglia development. Additionally, the neurological disorders resulting from NRROS deficiencies in mice demonstrates the crucial role NRROS plays in brain homeostasis and healthy CNS development.

Acknowledgements

I would first like to thank Professor Bin Chen, my faculty advisor, for providing the resources necessary to carry out this project.

I would also like to thank master's student Leora Huebner, and PhD student Kendy Hoang for teaching me the lab skills necessary to attain sufficient results for this project.

I would also like to thank PhD student David Tastad, PhD student Jeremy Tysporin, PhD student Yue Zhang, and PhD student Xiaoyi Liang for providing consultation whenever I ran into roadblocks.

Table of Contents

1. Introduction

The design goal of my senior thesis was to investigate and determine how the expression of *negative regulator for reactive oxygen species* (NRROS) in cells that constitute the innate immune system of the central nervous system (CNS) plays a critical role in establishing brain homeostasis, maintaining neuroplasticity, developing healthy synapses, and above all preventing early mortality. NRROS is a protein that enables immune cells to regulate their production of an inflammatory factor known as reactive oxygen species (ROS). NRROS is localized to the endoplasmic reticulum (ER), which is a continuous membrane system within the cytoplasm of eukaryotic cells and is important in the synthesis and transport of proteins. I had to set up mouse breedings to generate genetically modified mice in which their CNS endogenous immune cells were *NRROS-deficient* (*Nrros-/-* mice), which was achieved by deleting the *nrros* gene using the Cre-Lox system. The essence of this research was to test and analyze what happens to the development of the brain when there is partial to no NRROS production in the CNS. If this research shows that a CNS environment lacking NRROS is associated with disruptions in neuron-glia signaling, then we are another step closer to the development of new therapies and

biomarkers for neuroinflammation and neurodegenerative disorders such as Alzheimer's disease, Parkinson's disease, and amyotrophic lateral sclerosis (ALS).

Reactive oxygen species (ROS) produced by phagocytes are essential for host defence against bacterial and fungal infections. Excessive ROS can cause collateral tissue damage during inflammatory processes and therefore needs to be tightly regulated. NRROS is a myeloid-expressed transmembrane protein that regulates ROS production by enabling phagocytes, which are cells that are capable of engulfing and absorbing bacteria and other small cells and particles, to produce the required amount of ROS to clear invading pathogens, while minimizing unwanted collateral tissue damage. In the CNS, microglia are the specialized phagocytes that play a crucial role in brain inflammation, CNS homeostasis, and neuronal development. Additionally, they control clearance of cellular debris and uptake of glutamate and other neurotransmitters. Defects in microglial function have been associated with chronic neuroinflammation and disorders such as Alzheimer's disease, Parkinson's disease and amyotrophic lateral sclerosis (ALS).

Recently, our collaborators in the immunology department at Amgen reported that *Nrros*−/− mice developed spontaneous neurological disorders as they reached early adulthood, along with defects in motor functions. Motor defects seen were unstable gait, hunched posture, and limb paralysis. It was also reported that the mice died before 6 months of age. There data also showed that NRROS production in microglia cells is essential for microglial development and function. There appears to be an underlying NRROS-mediated molecular pathway that plays an important role in CNS development and function, however, this pathway remains poorly understood. I constructed my research around investigating the glial cells involved or effected by

the NRROS pathway, and to ultimately figure out why these NRROS−/− mice die at 6 months of age. To prepare for this project, I bred mice engineered to possess a condition where the expression of NRROS is completely nullified in their CNS immune cells, including microglia.

I constructed my research around surgically extracting brains of NRROS−/− adult mice and analyzing the cell population size and morphology of an aggregate of distinct cell types in brain. Once phenotypes such as paralysis in the hindlimbs and weight loss were observed in NRROS−/− adult mice, I perfused these mice and extracted their brains. It was important to extract the brain while maintaining the integrity of the cells that made up the brain tissue. After perfusions, I cryostated the brains, a method that involves an apparatus that can section the brains into thin slices. These sections ranged between 25 μm to 50 μm in thickness, which was crucial in order for antibody stainings to work. Subsequently, I mounted these thin brain sections onto a glass slide and conducted antibody stainings, a technique that allowed for targeting different cell type populations in the brain. Antibody stainings followed by subsequent imaging via fluorescence microscopy of these brain sections provided me with both the quantity and physical makeup of particular brain cells I was interested in studying. I will was able to capture and interpret the condition of these cells. The cells I stained for were glial cells, also called neuroglia, which are the most abundant branch of cell-types in the CNS. Glial cells are a bevy of non-neuronal cells in the CNS that function simultaneously to maintain healthy brain development. The glial cells that I stained for and investigated were microglia, astrocytes, and oligodendrocytes. I took the data collected from these cells observed in the mutant NRROS−/− mice brains and compared them to the glial cells of heterozygous mouse brains (partial NRROS expression). Studying neuroglial cells affected in an NRROS-deficient environment, and

understanding the differences observed in these cells (between the heterozygous brains and mutant brains) could further support our knowledge of the hitherto unknown NRROS pathway that seems to play a critical role in CNS homeostasis.

2. Background

2.1. Reactive Oxygen Species generation under physiological and pathophysiological conditions

2.1.1. Radicals and Reactive Oxygen Species (ROS)

Radicals are a chemical species with an unpaired electron in its outer orbit. Unpaired valence electrons are what give radicals their unstable and highly reactive nature. There are an array of radicals, but the most prominent type in biological systems are derived from oxygen, and are known collectively as *reactive oxygen species* (ROS). Oxygen has two unpaired electrons in separate orbitals in its outer shell, and this electronic structure makes oxygen especially susceptible to radical formation. ROS play a crucial role in reactions essential to life. Despite their beneficial activities, ROS are able to damage and adversely alter all macromolecules, including lipids, proteins, and nucleic acids, making them toxic for your cells (Robinson, 2008). Under *oxidative stress*, ROS is overproduced, which overwhelms the body's ability to regulate collateral tissue damage, triggering autoimmune disorders (Noubade, 2015).

2.1.2. Production of ROS in the human body

ROS are generated normally in physiological conditions and abnormally in pathological conditions. It has become overwhelmingly clear that ROS (in low concentrations) are involved in a myriad of physiological cell signaling pathways, referred to as redox signaling pathways (André-Lévigne, 2017). A well understood redox signaling pathway is oxidative phosphorylation in the electron transport chain (ETC), which is an important process for high-energy ATP production. The ETC is made up of a series of electron transporters known as *NOX* enzymes, which make up membrane-bound complexes that transport electrons across biological membranes (Morgan, 2003). During ATP production, the membrane-bound complexes are functional and situated inside of the mitochondrial inner membrane (Morgan, 2003). Four electrons are passed rapidly via an aggregate of electron carriers from one component to the next, to the endpoint of the chain where the electrons reduce molecular oxygen, producing two water molecules. The sequential reduction of oxygen (addition of electrons) leads to the formation of a group of intermediate ROS. The structures of the partially reduced oxygen radicals are shown in Figure 1. The addition of one electron to diatomic oxygen (O2) yields a superoxide anion (O2-). Addition of a second electron forms a peroxide (O2-2). Subsequently, a third electron creates a hydroxyl radical (OH), which is the most reactive radical intermediate. The addition of four electrons gives you water.

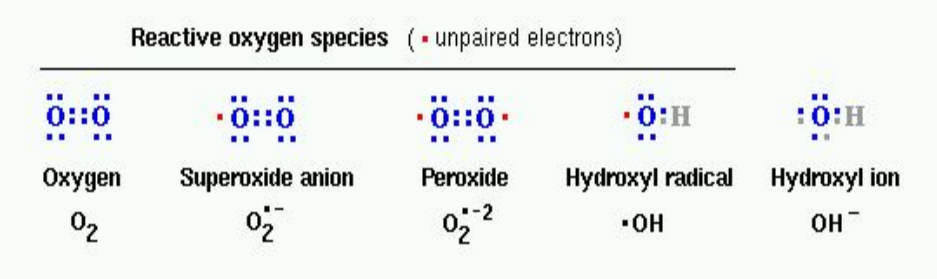

Figure 1: Atomic structures of ROS

Illustrated are the oxygen derivative molecules that are classified as ROS. These ROS intermediates arise in a multitude of biological pathways, such as aerobic catabolism of glucose via the electron transport chain. When diatomic oxygen gets a single electron it becomes superoxide anion, if it gets two electrons it becomes hydrogen peroxide, and then three electrons gives the hydroxyl radical. The addition of four electrons gives you water. The hydroxyl free radicals are generally the most reactive, making them the most damaging to your cells.

The production of ROS can also take place under pathological conditions. One way is through ionizing radiation, where the radiation penetrates tissue and knocks off an electron, generating a hydroxyl radical, which is an OH molecule with an unpaired valence electron. Another mechanism is your body's way of killing off invading pathogens, clearing out dying cells, and scavenging for foreign molecules. This is known as a proinflammatory response. Phagocytes are immune cells that protect the body by ingesting harmful foreign particles, bacteria, and dead or dying cells, and producing ROS to degrade them. Upon inflammatory stimulation, phagocytes travel to the site of an infection and ingest the invading pathogen. As they engulf harmful molecules, phagocytes simultaneously activate an immune factor complex known as *nicotinamide*

adenine dinucleotide phosphate (*NADPH*) *oxidase*. NADPH oxidase is made up of proteins that are similar to the ones that make up the complexes in the ETC (Bedard, 2007). NADPH oxidase is comprised of two membrane-bound subunits, allowing it to be functionalized in the membrane of phagocyte cells during the immune response (Bedard, 2007). Phagocytes use the NADPH oxidase to consume oxygen and rapidly convert it to superoxide (O_2^-) through NADPH oxidase-mediated process called *oxidative burst*, where a copious amount of ROS is produced. Pathogens are eliminated via superoxide release, which undergoes transformation into hypochlorite (bleach) (Morgan, 2003). This mechanism is illustrated in Figure 2.

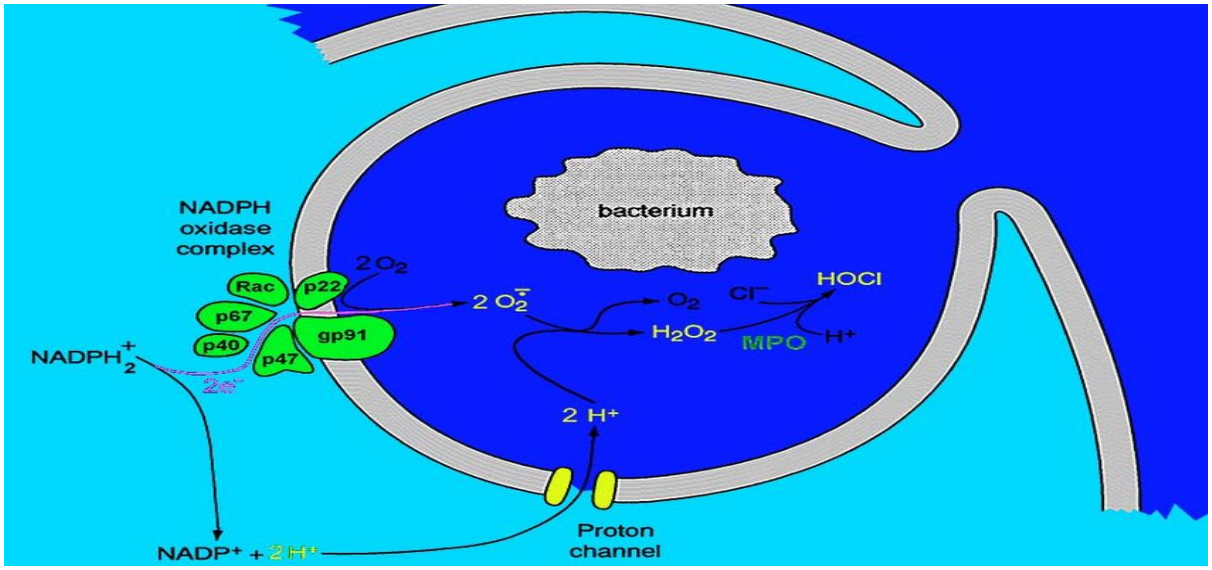

Figure 2: NADPH oxidase role in pathogen termination

The diagram shows the NADPH oxidase complex in the membrane of a phagosome in a phagocyte. The bacterium is in the center of a phagosome, which is closing around it. Gp9$_{phox}$, also known as NOX2, and p22$_{phox}$ are two subunits of the enzyme that reside in the membrane, whereas the other four subunits (p67$_{phox}$, p47$_{phox}$, p40$_{phox}$, and Rac) reside in

the cytosol (Morgan, 2003). When the NADPH oxidase enzyme is activated, the cytosolic components assemble with the membrane-bound components to form a functional enzyme. NADPH is then oxidized resulting in two electrons that are passed through the enzyme complex to extracellular O2. This creates superoxide (O2-), which transforms spontaneously into H2O2, which in turn is converted to hypochlorite by an enzyme myeloperoxidase (MPO) (Morgan, 2003). These reactive oxygen species, especially HOCl, participate in the killing of bacteria. (Morgan, 2003).

Deficiencies in regulation of inflammatory-produced ROS induces collateral tissue damage, accounting for all inflammatory diseases such as vasculitis, ischemic diseases, acquired immunodeficiency syndrome, etc (Lobo, 2010).

Levesque et al. (2013) research studied the correlation of air pollution to neuroinflammation and how this leads to central nervous system (CNS) damage. Levesque (2013) found that exacerbated ROS activity underlies *neurotoxicity*, which refers to toxin-causing damage of nerves in brain/spine (central nervous system) or peripheral nervous system (PNS), that can lead to Parkinson's and Alzheimer's.

2.2. Negative Regulator of Reactive Oxygen Species (NRROS) and its function

As discussed earlier, multicellular organisms employ ROS as mediators to enable a bevy of biological pathways. Excessive ROS leads to the development of

autoimmune diseases, underscoring the necessity of regulatory mechanisms that modulate ROS production. Our collaborator at Rajkumar Noubade, at Amgen, and his team have identified a significant mechanism that stabilizes ROS production during inflammatory responses (Noubade, 2014). Noubade and his team describe a protein, Negative Regulator of Reactive Oxygen Species (NRROS), which limits phagocytic competence to generate ROS during inflammatory responses. Noubade explains that NRROS regulates ROS production by directly interacting with *NOX2* (gp91*phox*), which is one of the membrane-bound subunits that make up the NADPH oxidase complex and plays a key role in phagocytic ROS production during oxidative burst. NRROS functions in the endoplasmic reticulum (ER) of cells, exploiting the ER-associated degradation pathway to facilitate the degradation of developing NOX2. Noubade also explains the role of another player in this pathway. Noubade found that NRROS competes with another enzyme known as p22*phox*, which binds to developing NOX2. NRROS-bound NOX2 induced trafficking to the ER-associated protein degradation pathway (Noubade, 2014). In contrast, p22*phox*-bound NOX2 stabilized NOX2, allowing for subsequent trafficking and assembly of functional NOX2 at the plasma membrane for ROS generation. This is schematically summarized in Figure 3.

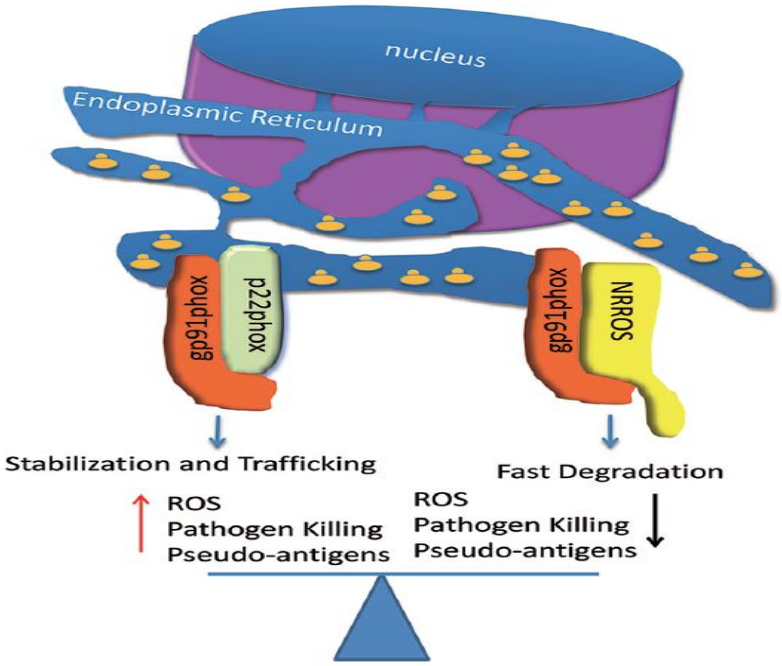

Figure 3: Nascent NOX2 Interaction in the ER

NOX2 is a major source of superoxide radical anions during phagocytic cell activation. Interaction of NOX2 with p22phox stabilizes NOX2 in the endoplasmic reticulum and allows for the maturation and trafficking of NOX2 to the plasma membrane where it becomes functional. NRROS competes with p22phox and is another NOX2-binding partner in the ER. Binding of NOX2 by NRROS accelerates NOX2 degradation, and thereby modulates ROS production by reducing NOX2 level.

(Bonini, 2014)

2.3. Glial Cells in the Central Nervous System (CNS)

2.3.1. What are Glial Cells

Glia are non-neuronal cells that were first identified by the 19th century's leading neuroscientists including Rudolf Virchow, Santiago Ramón y Cajal and Pío del Río-Hortega (Jäkel, 2017). At that time, glia cells were considered as purely non-functional glue for neurons, so-called "Nervenkitt" (the German word for nerve glue) (Jäkel, 2017). This is also reflected in the name "glial cell" derived from the ancient Greek word "glía" meaning "glue" in English (Jäkel, 2017). According to Chung (2015), glial cells are increasingly recognized to play a critical role in the health and function of the brain. Glial cells maintain and support neuronal homeostasis by influencing synapse development, plasticity, and function (Chung, 2015). Importantly, glial cell dysfunction has recently been shown to contribute to various neurological disorders, such as autism, schizophrenia, pain, and neurodegeneration (Chung, 2015). Understanding the function of glial cells under normal, physiological conditions, as well as how they goes awry in disease, has the potential to revolutionize how we understand the function and dysfunction of the CNS (Jäkel, 2017). Researching the pathways of how glia cells influence the immunology of the CNS will inspire the development of new therapies to treat these devastating disorders. There are four types of neuroglia cell lineages in the CNS, and they are *microglia*, *astrocytes*, *ependymal cells*, *oligodendrocytes*.

2.3.2. Microglia and CNS Macrophages

Microglia cells are the only tissue-resident macrophage in the central nervous system (CNS). However, they are a part of an aggregate of specialized macrophages that all constitute the innate immune system of the CNS. The other macrophages in the CNS are the choroid plexus macrophage, perivascular macrophage, and meningeal macrophages. These three macrophages are not situated in the tissue of the brain or spine like microglia, but they are located strategically in various anatomical niches of the brain (Herz, 2017). CNS macrophages not only provide an inflammatory role, they also have a multitude of functions, highlighting their substantial role in brain homeostasis and healthy brain development. They directly communicate with neurons, sample the blood in the brain, and clear amyloid-B molecules (Herz, 2017). According to Noubade et al. (2017), of all the cells that make up the brain and spine, CNS macrophages have highest NRROS expression, comparably. This makes sense since CNS macrophages possess phagocytic function.

Microglia originate from erythromeyloid precursors in the extraembryonic yolk sac (Kierdorf, 2013). According to Aguzzi (2013), microglia make up 10-15% of total brain cells. When a pathogen is detected, microglia go through a process called microgliosis, where they go from a steady state (basal state) into an activated inflammatory state. In an activated state, microglia are de-ramified causing a morphologically increased cell body (Stein, 2017). Activation of microglia produces an assortment of inflammatory factors. Over-activated microglia have a higher phagocytic behavior, over producing ROS and causing collateral CNS tissue damage. According to

Nimmerjahn's (2005) research, microglia withdraw from the activated state at the end of the repair but maintain a state of monitoring, confirming that microglial processes are dynamic and constantly sampling the environment. The varied morphologies of microglia is illustrated in Figure 4.

With the arrival of real-time imaging tools, microglia have erroneously been considered to be static bystanders in the healthy CNS that have minimal homeostatic functions besides phagocytic scavenging and immune surveillance (Li, 2018). Decades of research have highlighted the major role microglia play in regulating processes critical for neuronal development, maintenance of synapses, and injury repair (Herz, 2017). Given their vital role in normal brain function, it is not surprising that microglia dysfunction can be linked to neurological disorders.

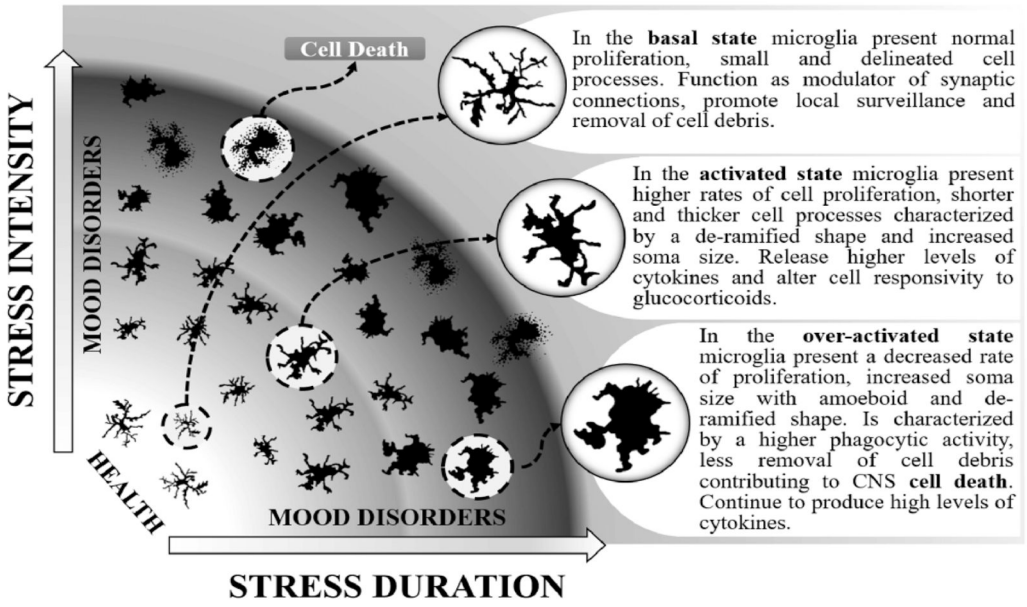

Figure 4: Different stages of microglia activation

Microglia are dynamic and constantly monitor the CNS environment. Their morphology indicates what state they are in. Small delineated (ramified) cell body with thin branching

processes means that microglia are in a steady state. In a steady state, microglia are surveying their surroundings and modulating synaptic connections. In an activated state, microglia have a larger cell body and thicker branching. In an activated state microglia release higher levels of cytokines. Over-activated microglia have a heightened phagocytic activity, which leads to collateral CNS cell death.

(Stein, 2017)

2.3.3. Astrocytes

Astrocytes are the most abundant and diverse neuroglia in the CNS, and yet there is no uniform and unequivocal definition of an astrocyte (Liddelow, 2017). However, because of their high abundance, astrocytes are the best studied and most well described glial cell population in the CNS. Conceptually, astroglial cells are as heterogeneous as neurons, and astrocytes in different brain regions may have very different physiological properties (Jäkel, 2017). Won-Suk Chung (2015) states that astrocytes have numerous processes and directly interact with various cellular structures in the brain and spine. The scope of astrocytic function involves the following: participate in trophic support of neurons, provide synapse maintenance, and prune synapses via phagocytosis, and also maintain brain homeostasis.

Due to their constant physical association with synapses and blood vessels, shown in Figure 5A, astrocytes act as a neurovascular bridge that provides neural circuitry with blood flow required for metabolic processes

(Harada, 2016). Astrocytes have a highly dynamic behavior to enable the modulation of synapses, axons, and blood vessels during development and adulthood, controlling the connectivity of neuronal circuits (Chung, 2015).

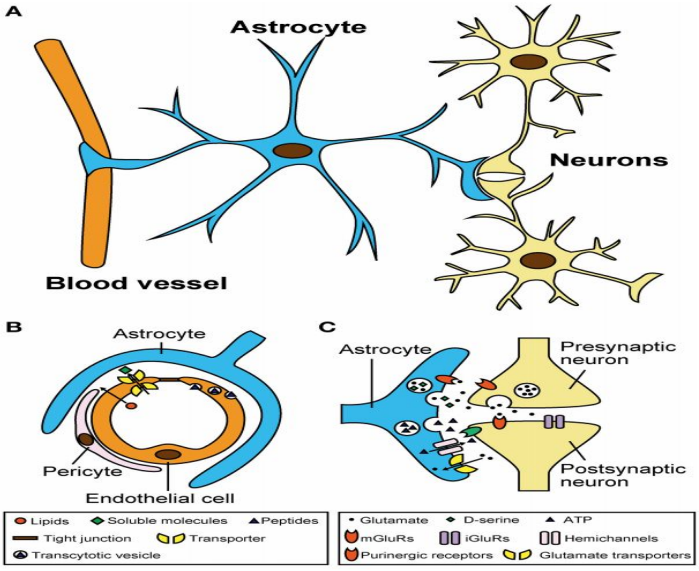

Figure 5: Astrocytes have close morphological and functional associations with blood vessels and neurons

5A depicts how astrocytes have close morphological and functional associations with blood vessels and neurons. The end feet of astrocytes are bound to blood vessels and neurons, integrating neural circuitry with local blood flow and metabolic support. The astrocyte illustrated is therefore at a strategic position, with one arm at the blood vessel, with its other at the neuronal membrane, synapse or axon. It can thus be viewed as the neurovascular bridge. 5C illustrates astroglial glutamate transport, which is crucial for neuronal glutamatergic transmission by operating the glutamate–glutamine shuttle. Glutamate is the major excitatory neurotransmitter in the nervous system. Research has shown that microglia directly

communicate with astrocytes, and so microglial dysfunction leads to the development of a deleterious reaction known as astrogliosis, which is an abnormal increase in reactive astrocytes. (Harada, 2016)

Astrocytes create the brain environment, build up the microarchitecture of the brain parenchyma, maintain brain homeostasis, store and distribute energy substrates, and provide aid for brain defense (Jäkel, 2017). They also control the development of neural cells, and recent findings have implicated that astrocytes play a primary role in synapse formation and elimination, as well as synaptic plasticity, which is the change that occurs at synapses (the junctions between neurons that allow them to communicate) (Chung, 2015). Observed in Figure 5C, astrocytes play a crucial role in glutamate transport, which is crucial for neuronal glutamatergic transmission (neuronal impulse communication). It is therefore likely that defects in astrocyte function contributes to the initiation and progression of neurological disorders (Chung, 2015). A familiar morphological sign of defective astrocyte function is *astrogliosis*, which is is an abnormal increase in the number of reactive astrocytes in CNS tissue due to the destruction of nearby neurons from CNS trauma, infection, autoimmune disorder, and neurodegenerative disease. According to Wyss-Coray (2012), microglial activation and reactive astrogliosis are linked events, indicating their ability to directly communicate, and they are both hallmark features of Alzheimer's disease

(AD) and other neurodegenerative diseases (NDDs), including Huntington's disease and Parkinson's disease.

2.3.4. Oligodendrocytes

Oligodendrocytes are the myelinating cells of the central nervous system (CNS). Myelin is a mixture of proteins and phospholipids that forms a whitish insulating sheath around many nerve fibers. Myelin insulation increases the speed at which impulses are conducted and sent to other neuronal cell bodies. According to Monika Bradl (2009), oligodendrocytes are the end product of a cell lineage, which has to undergo a complex and precisely timed program of proliferation, migration, differentiation, and myelination to finally produce the insulating sheath of axons. Due to this complex differentiation program, and due to their unique physiological function, oligodendrocytes are among the most important and vulnerable cells of the CNS (Bradl, 2009).

2.4. What are Cre-Recombinase Transgenic Mice

The *Cre/loxP* recombination system is the most robust approach to produce cell-type-specific gene inactivation (Parkitna, 2009). The selectivity and reproducibility of Cre expression is absolutely critical for acquiring valid results. For example, if scientists who want to observe what happens to the liver of a mouse when a specific protein is not expressed, they would use the Cre/loxP system to deactivate the expression of this protein only in liver tissue. Cre/loxP recombination substantially mitigates

misleading results that could be caused by the loss of this particular protein in another tissue type.

Observed in Figure 6, the knockout of GeneX takes place when the Cre recombinase is expressed from a transgene containing a tissue-type-specific promoter (K. Peter 2016). In Figure 6, Alb is the tissue-specific gene that is only expressed in the liver and would be that gene downstream of the promoter. Along with Alb, cre recombinase will also be expressed and functionalized because it is downstream the same promoter because it is ligated next to Alb (K. Peter 2016). Expressed Cre recombinase will execute its function and delete genomic segments flanked by loxP sequences in this tissue only (K. Peter 2016). Any GeneX with a loxP sequence on both sides in the genome of liver-resident cells would have no expression of GeneX because it would be deleted (K. Peter 2016).

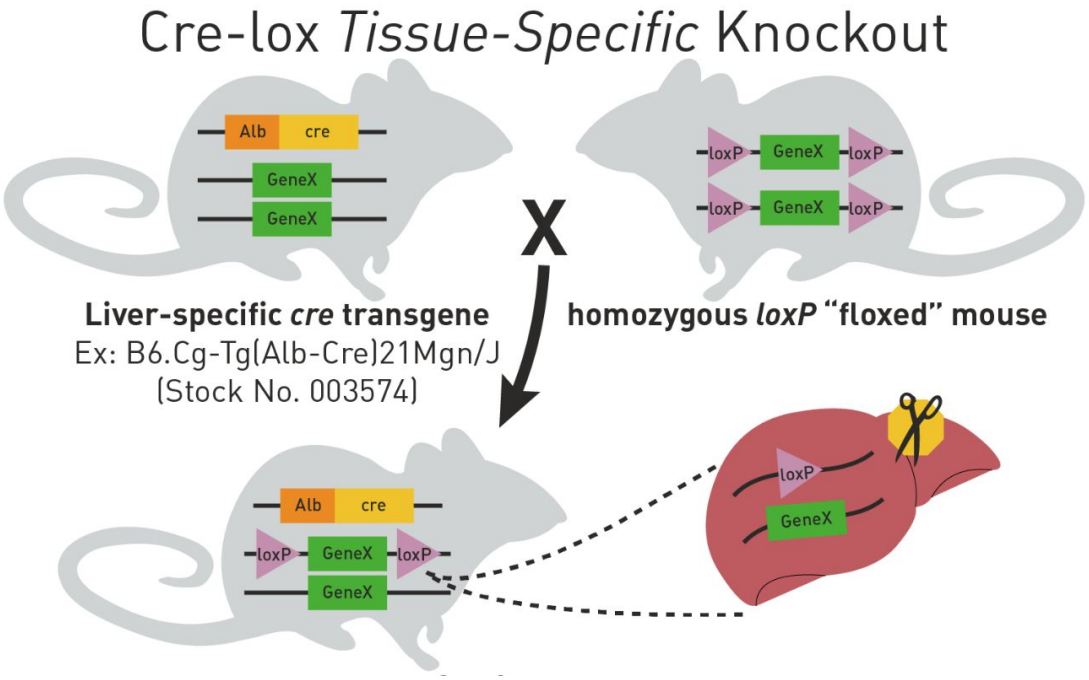

Figure 6: Mouse breeding setup heterozygous knockout for GeneX via Cre-lox system

Mate Alb cre mice with homozygous loxP-flanked mice will result in approximately 25% of the progeny from this mating to be homozygous for the loxP-flanked allele and heterozygous for the cre transgene. Meaning that liver cells will have a decreased ability to express GeneX because expressed Alb-cre recombinase expression will cut out GeneX DNA sequence when it has a loxP sequence on both sides of it.

(K. Peter 2016)

2.5. Prior Research on NRROS-deficient mice

Rajkumar Noubade and his team at Amgen have studied NRROS-deficient mice (Noubade, 2017). They knocked out NRROS expression in CNS macrophages, which include microglia, via CX3CR1 cre-recombination. CX3CR1 is a chemokine receptor that is expressed by CNS resident macrophages, and its ligand is a neuron-expressed molecule known as CX3CL1. CX3CR1-CX3CL1 is a macrophage-neuron communication pathway that plays a role in synaptic pruning (Noubade, 2017). Mice were considered mutant when CX3CR1 producing cells had NRROS floxed out and deleted, resulting in their CNS macrophages lacking the ability to express NRROS. Mutant (NRROS -/-) mice developed spontaneous neurological disorders after 8 weeks of development, indicated by hindlimb paralysis. NRROS-deficient mice also displayed bladder incontinence, where they had involuntary bladder discharge and ensuing toxin build up in their bladders. Ultimately, these mice did not live past 6 month. The molecular cause of these phenotypic defects is still unknown.

3. Work Done

3.1. Objectives

The objective of my research was to investigate what CNS cells and pathways undergo detrimental modifications in mice that have NRROS absent in their CNS environment. Our collaborators at Amgen, Rajkumar Noubade et al., observed unstable gait, hind limb paralysis, hunched posture, urinary incontinence, and early mortality (6 months of age) in NRROS-deficient mice. Prior to the emergence of these phenotypes, NRROS mutant mice displayed normal development up until around 8 weeks of age.

These symptoms suggested underlying neurological defects associated with Multiple Sclerosis (MS). MS is an autoimmune disease that attacks the myelin wrapped around nerve fibers causing nerve damage, attenuating and crippling CNS communication with muscular motor neurons throughout the body. To further study these phenotypes, Rajkumar Noubade and his team utilized Cre-Lox technology and generated a mouse line that had NRROS deleted in their peripheral myeloid populations. Targeting NRROS deletion in these peripheral myeloid populations was driven by lysozyme (Lyz2-Cre), a mouse model for MS.

Surprisingly, our collaborator's CNS histological studies, displayed in Figure 7a, showed no inflammatory infiltration of the spinal cord or brain, which is a hallmark of T-cell mediated *experimental autoimmune encephalomyelitis* (EAE). EAE is an inflammatory demyelinating disease of the CNS and serves as an effective experimental

animal model for MS. In addition to this finding, our collaborators also conducted a p-phenylenediamine staining of the sciatic nerves to compare the axon myelin sheath between WT and NRROS-/- mice. The results showed similar degrees of myelination in WT and NRROS -/- mice, as reflected by the percentage of axon-lumen area per nerve area (seen in Figure 7b&c). Total numbers and density of axons were also similar between WT and mutant mouse strains. Although the physical phenotypes displayed by NRROS -/- mice are comparable to signs observed in mice with MS, the data collected by our collaborators suggests that the absence of NRROS does not give rise to the defects seen in MS.

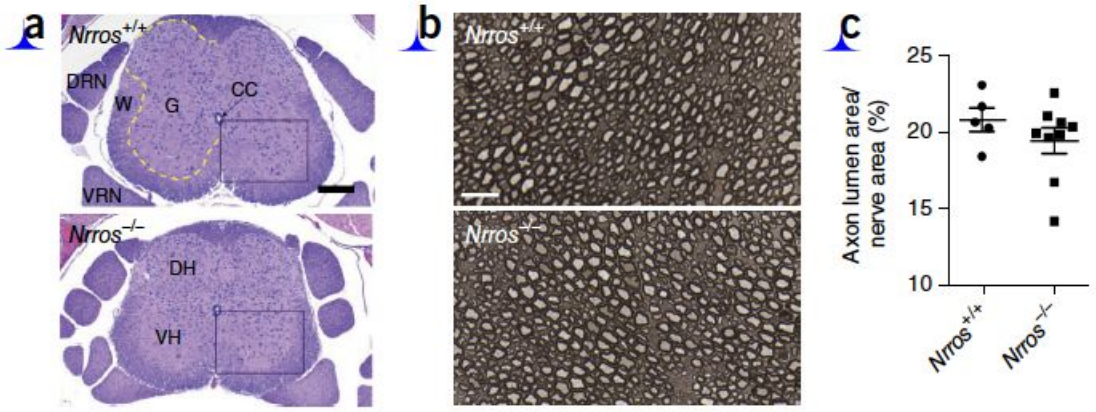

Figure 7: Collaborator's results from assays testing for signs of MS defect phenotypes

*(**a**) Hematoxylin and eosin staining of spinal cord cross-sections from WT and Nrros−/− (KO) mutant mice. Comparisons of WT and mutant stainings show no inflammatory infiltration of spinal cord in the NRROS-deficient mice. (**b**) Images from p-phenylenediamine staining assay of cross-sections of sciatic nerves from WT and KO mice. Results present similar degrees of myelination in WT and NRROS -/- mice, as reflected by the percentage of axon-lumen area per nerve area. The scale bar is 10 µm. (**c**) Percentage axon lumen area per nerve area (n = 5 WT, 9*

KO). Total numbers and density of axons were also similar between WT and mutant mouse strains. The results of these assays indicate that although the physical phenotypes displayed by NRROS -/- mice are comparable to signs observed in mice with MS, the absence of NRROS does not generate characteristical defects in MS.

(Noubade, 2017)

Our collaborators asked my Principal Investigator (PI), Bin Chen, for help in finding the defect that causes early mortality in NRROS-deficient. After hearing about the opportunity for the Bin Chen lab to work on this project, I asked Bin Chen if I could be selected to work on this project. Our collaborators provided my lab with four CX3CR1-cre/+ female mice and two male mice that were NRROSFL/+ and another two males that were NRROSFL/FL.

3.2. Methodology

3.2.1. *Breeding and Tagging WT, Heterozygous, and Mutant Mice*

Due to vivarium rules, the mice had to be placed in the quarantine room for 3 months. I set up four F0 breeding cages, a female and male in each one. I recorded the genotypes being crossed and waited until the females were pregnant. Once the litter dropped, I recorded the date they were born, reported as the P0 date. At around 3 weeks of age, I separated the F1 progeny from their parents and set up another F0 breeding cage. I placed all the F1 males in one cage and F1 females in another to prevent any chance of ending up with pregnant females and not knowing which male they mated with. Before allocating each mouse to its

respective cage during separation, they were tagged. Shown in Figure 8 are the tools used to properly tag mice.

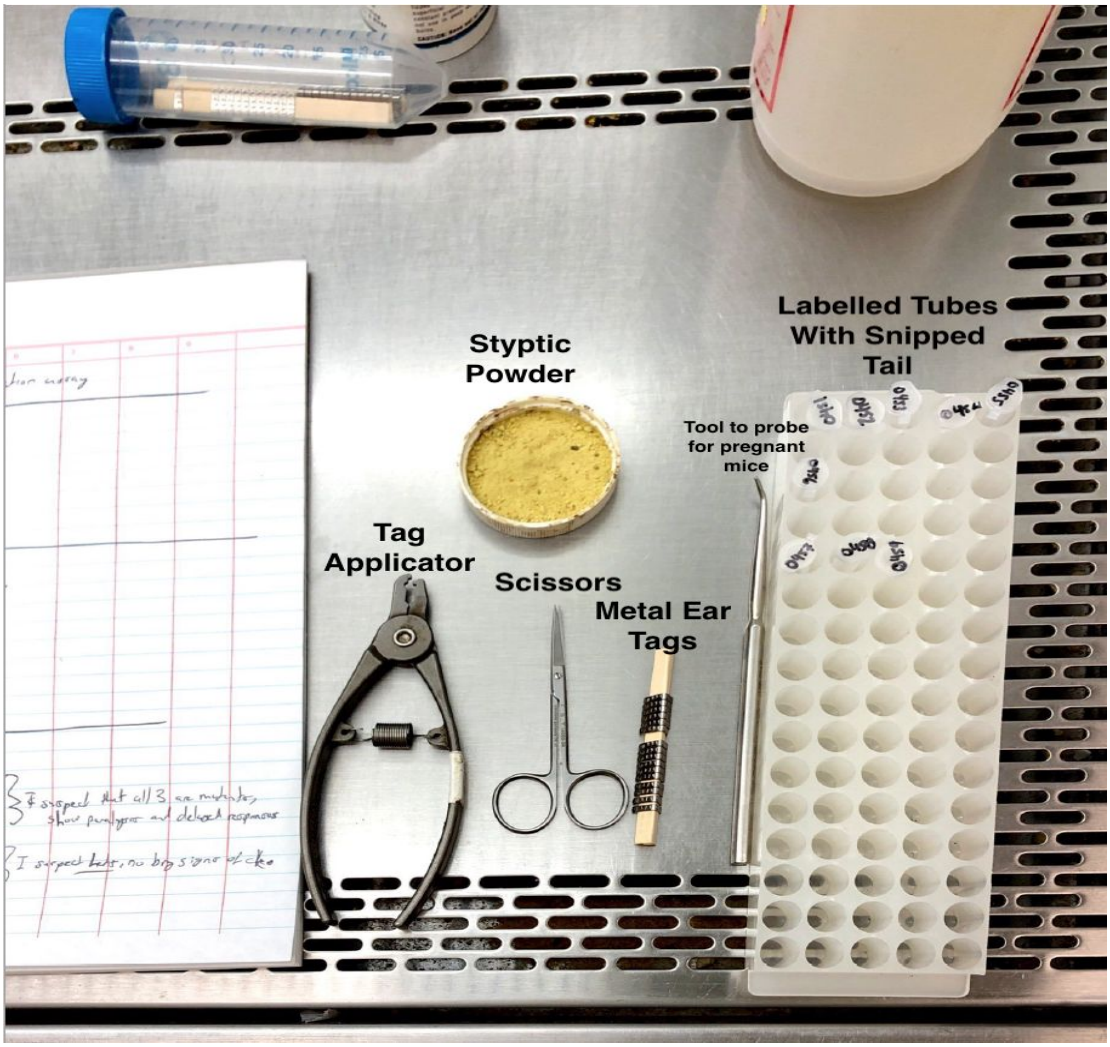

Figure 8: Tools for tagging mice

The gender, fur color, and tag number for each mouse was recorded in my lab notebook. A metal ear tag with an engraved number was clipped onto the ear of each mouse using a stainless steel tag applicator. Next, I snipped off the end of their tail using a sharp pair of scissors, and transferred the small portion of the cut tail into a 1.5 mL eppendorf tubes. The tail of each mouse was cut for the purpose of purifying their DNA, which is required in order to know their

genotype. Styptic powder was immediately applied to the site of laceration where the tail was snipped to stop the bleeding.

A metal ear tag with an engraved number was clipped onto the ear of each mouse using a stainless steel tag applicator. After, I snipped off the end of their tail using a sharp pair of scissors, and placed the small portion of the cut tail into a 1.5 mL eppendorf tubes. The tail of each mouse was cut for the purpose of purifying their DNA, which is required in order to find out their genotype. A styptic powder was immediately applied to the site of laceration where the tail was snipped in order to stop the bleeding. Before leaving the mouse room, I made sure all the cages had enough food, were labeled correctly, and placed back onto the racks accordingly. During this time I would also check on my breeding cages to keep track of pregnant females, and/or check if a new litter dropped. I also had to make sure there was no cage overcrowding. A cage is deemed overcrowded if there are 3 adult females, an adult male, and a litter in one cage, or more than 6 adult mice in one cage. Not following these guidelines could result in a lab fine, hence I regularly checked on my cages for overcrowding.

3.2.2. *DNA Precipitations*

In order to genetically identify each mouse from the tagged progeny, I had to extract and purify the DNA from each tail snip sample, respectively. This process is called DNA precipitation. First, each tail sample is placed into a 1.5 mL eppendorf labeled with the tag number of the mouse the tail belonged to. Using a

P1000, I pipetted 500 µL of tail lysis buffer (see appendix A.3) and 7µl of proteinase K into each sample tube. Proteinase K is a broad spectrum serine protease and is used in many DNA extraction protocols to digest contaminating proteins and nucleases (enzymes that degrade nucleic acids). Next, I placed the samples into a 55°C incubator overnight. The samples were then vortexed and centrifuged at 15000 rpm for 1 minute. At this point, the DNA is in the supernatant, and 400 µL of the supernatant is extracted and pipetted into another labeled eppendorf tube with 1 mL isopropanol. The DNA-contained supernatant and the isopropanol were mixed together by inverting the 1.5 mL eppendorf tube. Next, the samples were centrifuged at 15000 rpm for 10 minutes. At this point, the DNA is the pellet at the bottom of the eppendorf tube, so the supernatant is dumped out and 400 µL of 70% ethanol was pipetted into the sample (to wash off excess NaCl) and centrifuged again at 15000 rpm for 10 minutes. Next, a transfer pipette with a p200 pipette tip was used to suck out the 70% ethanol, while avoiding the DNA pellet at the bottom. The sample tubes were left open and placed in the 55°C incubator for 15 minutes to evaporate any excess ethanol. Finally, 500 µL of nano-pure water was pipetted into each labeled sample eppendorf tube. The next step was to analyze the genotype of the mice by putting their purified DNA through polymerase chain reaction (PCR).

In situations where no DNA band showed up for a particular sample after PCR and gel electrophoresis, I would analyze the DNA concentration of the sample via NanoDrop. A NanoDrop is a spectrophotometer that allows for quick

and easy quantification of the nucleic acid concentration in samples after DNA precipitation. The recommended concentration is 100 nanograms (ng) of nucleic acids per 1μL of solution (100ng/μL), which consists of nano-pure H2O and DNA. Observed in Figure 9 is the Thermo Fisher NanoDrop I used to check DNA sample concentrations. First, I washed the sensor three times with 1 μL of nano-pure H2O, in between each step a kimwipe was used to dry the sensor. Next, I turned on the software required for concentration quantification. I blanked the sensor with nano-pure H2O and proceeded to pipette 1 μL of DNA sample from the 1.5 μL eppendorf tube. In between each sample recording, I dried of the sensor with a kimwipe. If DNA sample concentration was too high (significantly greater than 100ng/μL), I would compensate by pipetting more nano-pure H2O into the 1.5 mL eppendorf tube. In situations where a sample had low DNA concentration, I would pipette more DNA into the PCR tubes during PCR preparation.

Figure 9: Thermo Fisher NanoDrop

Pictured here is NanoDrop device used to check the concentration of DNA after DNA purification. 1 µL of DNA from the eppendorf was pipetted into the sensor pore. Afterwords, I closed the lever and used the software to compute the concentration of DNA in the sample (nanograms/ µL). The desired concentration before proceeding with PCR was 100 ng/µL.

3.2.3. *Genotyping by PCR and Gel Electrophoresis*

PCR is a popular technique used to identify and amplify a DNA target sequence in a sample of DNA. PCR was the method I used to determine whether a mouse from the progeny was WT, heterozygous, or mutant. PCR enables an accurate amplification of targeted DNA sequences; specifically DNA sequences encoding for CX3CR1 and NRROS for my research.

Prior to placing the samples into a PCR thermocycler, I needed to mix the purified DNA samples with the adequate PCR master mix. The master mix was a blended concoction of the following: 10X PCR buffer (see in appendix A.2), MgCl2, dNTPs, Taq polymerase, and the required primers to target the DNA sequences of NRROS and CX3CR1cre. The volume of master mix prepared depended on how many samples I had to run on the PCR thermocycler (see in appendix B.1). The master mix solution was contained inside a labeled 1.5 mL eppendorf tube. The two PCR primers that targeted and amplified the *nrros* gene were BC 1710 and BC 1711. Primers that targeted and amplified the *cx3cr1* gene were BC 1711, BC 1712, BC 1713, BC 1714. The final component added to the master mix was the Taq polymerase enzyme. Preceding the addition of Taq polymerase, I pipetted 3 µL of each purified DNA sample into a respective PCR tube. Upon subsequent addition of Taq polymerase to the master mix, I inverted the master mix solution and pipetted 20 µL of PCR master mix into each PCR tube containing 3 µL of purified sample DNA. The final preparation step was to spin down the PCR tubes in order to blend the master mix solution with the purified DNA. PCR tubes were placed into the thermocycler machine, shown in Figure 10, with a specific protocol for each genotype (see in appendix B.2). The PCR runs took approximately 2.5 hours to complete.

Figure 10: PCR Thermocycler

Pictured here is the thermocycler used to amplify the target regions of CX3CR1 and NRROS. After preparation and mixing of the master mix and sample DNA in PCR tubes, I placed the PCR tubes into the thermocycler. I entered the appropriate protocol for accurate DNA fragment amplification. (Protocols seen in appendix B.2)

Taq polymerase was the last component added to the master mix because it is a DNA polymerase and it has a chance of initiating the amplification reaction before adding the samples to the thermocycler. This would be an issue because the DNA will not have been denatured yet, nor will the primers have annealed to the target NRROS and Cx3cr1DNA sequence sites. A possible result of this could be non-specific synthesis, causing the amplification of random fragments during PCR in the thermocycler. Taq polymerase has a very high optimal temperature (75-80°C). However, this does not mean that the polymerase will not work at

lower temperatures (like room temperature), but instead means that it works best at higher temperatures. At lower temperatures the polymerase will still execute its function, but not as efficiently and as a result will be more likely to make a mistake during synthesis. In general, you should always add enzymes to a reaction last, to prevent them from working before they are needed.

Afterwards, I prepared a 2% agarose gel (see in appendix A.1) for gel electrophoresis in order to isolate and observe the amplified DNA fragments based off size. Gel electrophoresis was the method used for size separation and analysis of the amplified samples. I took the amplified DNA samples out of the thermocycler and added 7μL of orange loading dye. This step allows for the amplified DNA (represented as bands on an agarose gel) to be detected by the gel imaging system, shown in Figure 11. Next, the gel was submerged into a 1X TAE buffer solution and 25 μL of the amplified DNA & loading dye buffer solution was pipetted into the loading wells with a P200. I pipetted 5 μL of a 1 kb DNA ladder at the end of each row on the gel in order to identify the size of the DNA bands in each lane. After loading the gels, I placed the lid on and ran the gel electrophoresis machine at 180V with a current of 300 mA for 20 minutes. The voltage difference is established by two electrodes (positive and negative charge), generating an electrical current through the gel. Due to the uniform negative charge of DNA, DNA moves through the gel towards the positive electrode. The smaller the DNA fragment, the farther down the gel it travels.

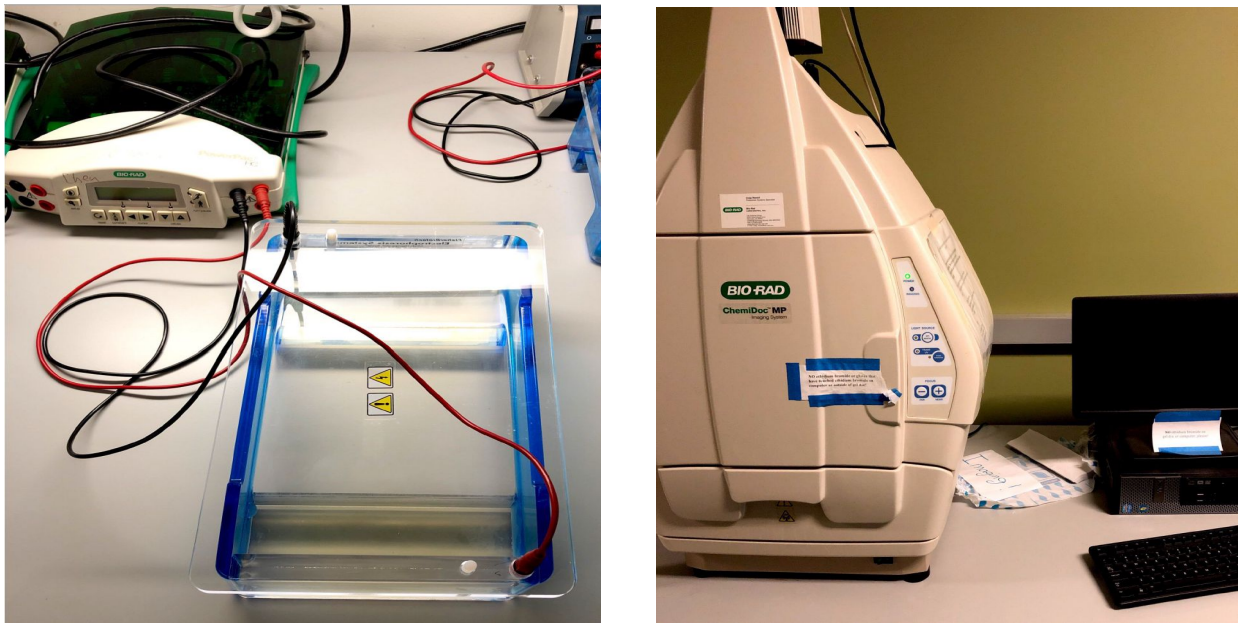

Figure 11: Gel Electrophoresis Instrument and Gel Imaging System

Shown on the left is the gel electrophoresis machine. The 2% agarose gel with its incised wells are loaded onto this machine and submerged in TAE buffer. The PCR products are mixed with orange loading dye and pipetted into the wells . When the machine is running with a voltage of 180V, the DNA in the wells will electrophoretically translocate down the gel towards the positive electrode (red). The smaller DNA fragments move farther down the gel than the larger fragments. The machine is run for 20 minutes. Next, the gel is imaged the gel imaging system (right). The PCR products of my target sequence are visualized after the gel is imaged. The image is saved onto the computer for record keeping.

Depending on the size of the target region from the amplified sample, I was able to tell whether the mice are CX3CR1cre/+, NRROS FL/+ (heterozygous) or CX3CR1cre/+, NRROS FL/FL (mutant). If the mice are missing one of the bands representing CX3CR1cre/+ or NRROS FL/*, then they

are WT. Illustrated in Figure 12 are the genotypes of 2 different mouse progenies, providing a total of 31 samples. The WT band for CX3CR1cre is 302 bp, represented as the lower band, and the mutant band is 380 bp, represented as the higher band. The WT band means that the gene encoding for Cre recombinase is not present in the same transcriptional domain as CX3CR1. The mutant band tells me Cre recombinase is present in the same transcriptional region as CX3CR1, confirming the expression of Cre recombinase in CX3CR1 expressing cells. Looking at the gel in Figure 12, you can see how the samples exhibit either a WT band or both a WT and mutant band (heterozygous) for CX3CR1cre. This is because Cre recombinase only needs to be present on one of the two CX3CR1 alleles in order for the *nrros* gene to be floxed out (deleted) in CX3CR1-expressing cells, which is why the first set of female mice received from our collaborators were all CX3CR1cre/+ genotypes.

Displayed on the lower half of the gel in Figure 12 are the bands representing NRROS. The lanes containing CX3CR1 target amplification either have two bands of size 302 bp and 380 bp (CX3CR1cre/+ genotype), or one band of size 302 bp (WT genotype). Two bands present in lanes containing NRROS amplified DNA fragments of size ~450 bp and ~550 bp represent NRROS FL/+ heterozygous mice. Mutant NRROS FL/FL samples are characterized by a single band of size ~550 bp. Heterozygous mice have a genotype of CX3CR1cre/+ and NRROS FL/+, where essentially their CX3CR1-expressing cells have one of the two *nrros* alleles floxed and deleted. This will result in a partial expression of

NRROS in the CNS immune cells for these mice. Mutant mice have a CX3CR1cre/+ and NRROS FL/FL genotype, for these mice both *nrros* gene copies are floxed and deleted in all of their CX3CR1-expressing cells.

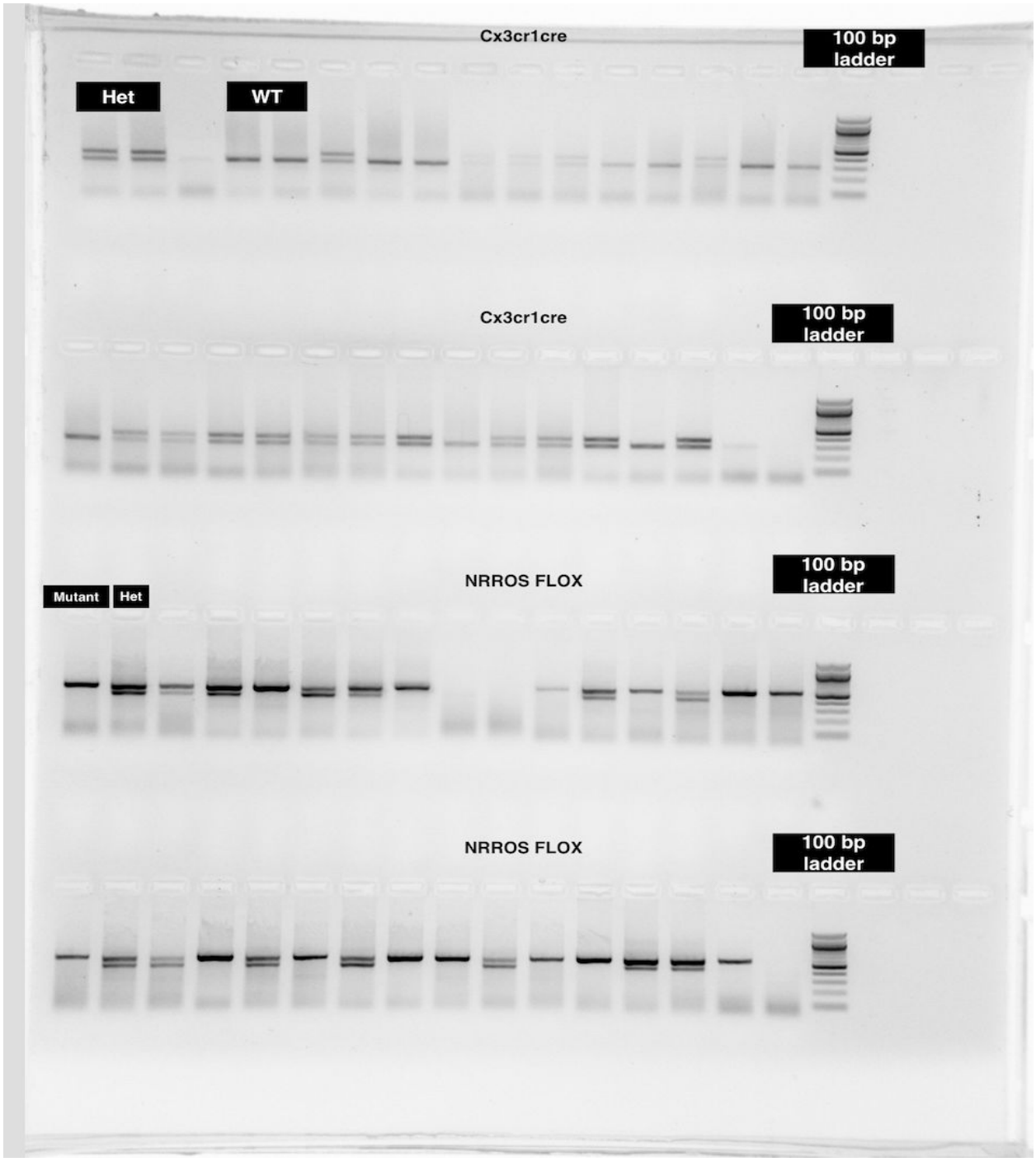

Figure 12: CX3CR1cre X NRROS Flox genotypes of mice after PCR

The image is obtained by the gel imaging system after running the gel containing the PCR products of CX3CR1 and NRROS. The first two rows are analyzing the band size of the cx3cr1 gene fragments and the second two rows are analyzing the band size of the nrros gene fragment. Each lane has its own sample and the lanes positioned in the same location in the CX3CR1 rows NRROS rows correspond to the same sample. Two bands present in lanes containing NRROS amplified DNA fragments of size ~450 bp and ~550 bp represent NrrosFL/+ heterozygous mice. Mutant NrrosFL/FL samples are characterized by a single band of size ~550 bp. The lanes containing CX3CR1 target amplification either have a two bands of size 302 bp and 380 bp (CX3CR1cre/+ genotype), or one band of size 302 bp (WT genotype). Heterozygous mice have a genotype of Cx3cr1cre/+ and NrrosFL/+, where essentially some (but not all) of their Cx3cr1-expressing cells have the DNA sequence for NRROS deleted. Mutant mice have a Cx3cr1cre/+ and Nrros FL/FL genotype, for these mice the nrros gene is deleted from all their Cx3cr1-expressing cells.

3.2.4. *Mouse Perfusions and Brain Extraction*

Brain perfusion is a surgical technique that allows for full brain extraction while maintaining the tissue integrity. Slicing the brain up into thin sections and probing these sections for specific cells via antibody stainings (immunostaining) allows for *in-situ* analysis of brain cells, meaning they have been preserved in their original environment. I wanted to compare and contrast the morphology and cell count of astrocytes, microglia, and oligodendrocytes, in the brain between the

NRROS-heterozygous and NRROS-mutant brains at a very late age where the neurological defects are conspicuous. I grew the mice to be around 3.5 - 4 months of age. This was done to allow for a comprehensive analysis of CNS neuroglial cells in an environment where NRROS -/- induced neurological disorders have fully manifested. Additionally, no one has observed the brains of NRROS-deficient mice that late in age. There were multiple F1 progenies that had reached the age threshold (3.5 - 4 months) at the same time. In the span of 2 weeks I perfused 40 mice and extracted their brains.

First, I prepared the set up required for mouse perfusions in the fume hood, shown in Figure 13. The surgery was done on a tray that had a passage to filter out the blood. A congeal platform was required for mounting and securing the mice in place. A needle for each limb was used to fasten the mice to the platform. A catheter (PVC high pressure tubing with luer ends) was needed for filtering the blood. The catheter had a perfusion needle connected to one end for insertion/transfer of reagents into the heart, and the other end was placed into a conical tube containing a particular reagent. The catheter was locked into a motor that allowed for a constant transfer of the particular reagent (1X PFA & 4% PFA) through the catheter. The largest pairs of surgical scissors and tweezers were picked out from the surgical kit because I was dealing with adult mice.

Reagents required for proper brain extraction were 4% paraformaldehyde (PFA) (seen in appendix A.4) and 1X phosphate-buffered saline (PBS) (seen in appendix A.5). PBS is a buffer frequently used in biological applications, such as

washing cells, transportation of tissues, and dilutions. 1X PBS closely mimics the pH, osmolarity, and ion concentrations of the human body. 1X PBS was injected into the apex via the perfusion needle and entered the left ventricle of the heart, allowing 1X PBS to circulate and replace all the blood in the mouse tissue. After all the blood drained and replaced by 1X PBS (indicated by a clear and bronze-like color exhibited by the liver), 4% PFA was injected for tissue fixation, which was a critical step in the preparation of histological sections. The broad objective of using 4% PFA is to preserve the integrity of cells and tissue components for structural investigation. PFA allows for increased mechanical strength and stability of tissue during sectioning and subsequent staining.

Before the surgery, the age, genotype, and weight of the mouse was recorded. Then they were anesthetized via 3 minute exposure to isoflurane. Afterwords, they were mounted and fixed onto the platform. The skin surrounding the chest was removed and an excision was made at the sternum. Both sides of the rib cage were cut and held at an angle with tweezers, exposing the heart. The right atrium was cut with one snip and the perfusion needle, twisted into one end of a peripheral venous catheter (PVC), was immediately inserted into the apex and pushed in just enough to enter the left ventricle of the heart. The other end of the PVC was submerged in the 1X PBS conical tube. The PVC was locked into a motor to establish a constant flow of 1X PBS and 4% PFA into the heart. Upon immediate insertion of the perfusion needle into the heart, the motor was turned on and 1X PBS flowed into the heart at a constant rate. Blood was filtered out and

replaced by 1X PBS. The needle was held steady for ~3 minutes (until all the blood exited the body). Next, I turned off the motor and switched the end of the PVC from the 1X PBS tube into the 4% PFA tube and turned the motor back on. The PFA circulated into the body at the same rate as 1X PBS. Every 30 seconds I flicked the head of the mouse to see how stiff it would get over time. Once the tail and head were stiff, I switched the end of the catheter into the 1X PBS tube and turned off the motor. Next, I removed the mouse from the platform and meticulously extracted the brain from the skull. This step was the most time consuming because I did not want to damage the brain while removing the skull with tweezers.

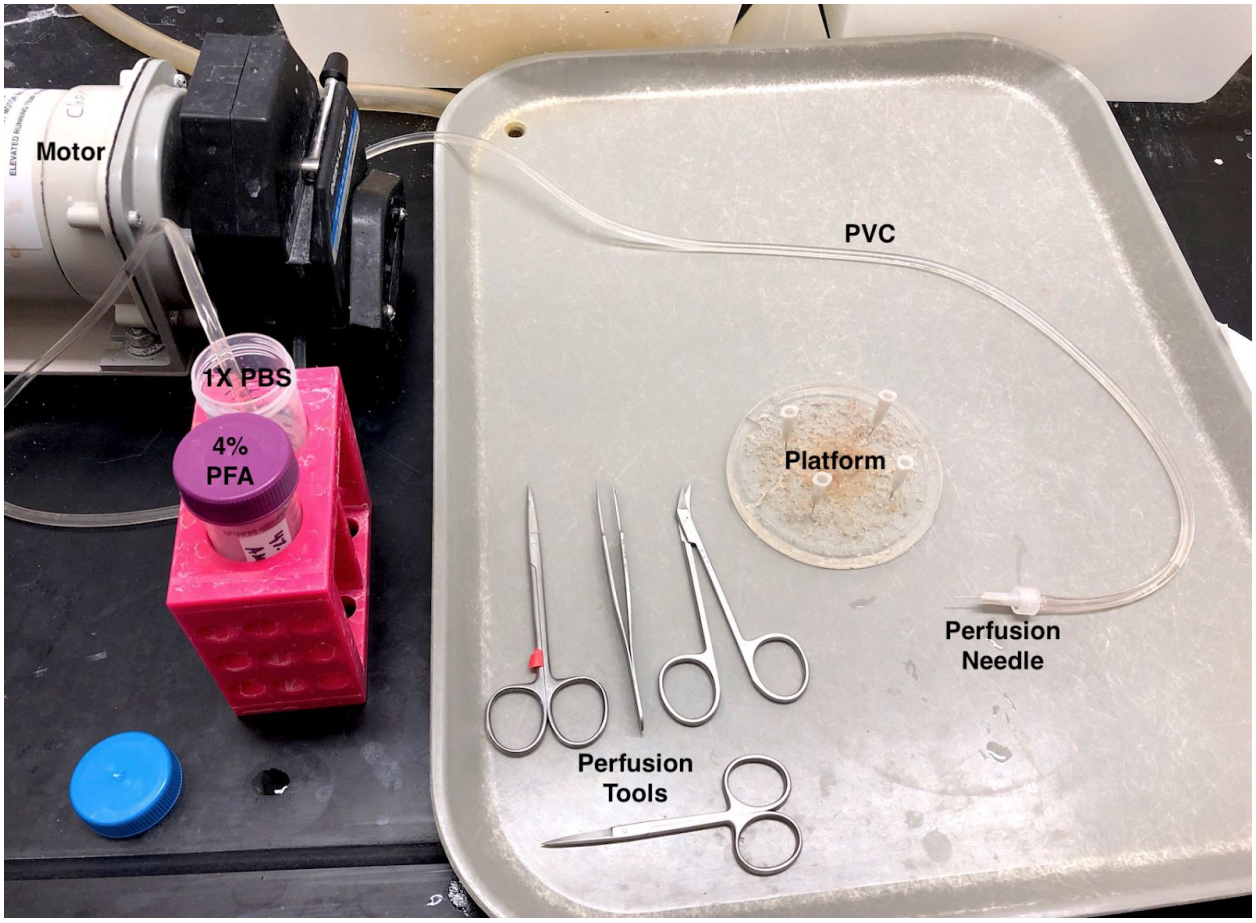

Figure 13: Profusion set up

Catheter tube with perfusion needle was needed for filtering blood out of the body and injecting reagents. Reagents required for proper brain extraction were 4% paraformaldehyde (PFA) (seen in appendix A.4) and 1X Phosphate-buffered saline (PBS) (seen in appendix A.5). Surgical scissors and tweezers were needed for perfusion and brain extraction. Congeal platform and 4 needles were used to fix the anesthetized mouse into place. Motor was required for steady flow rate of PBS and PFA into the heart. All perfusion were done on a tray with a channel in the top left to drain the blood.

Prior to perfusion and brain extraction, I prepared and labeled a 12 well plate (seen in Figure 14). I wrote the P0 date, perfusion date, mouse tag number,

mouse genotype, and brain number in the order they were extracted on the 12 well plate. I pipetted 1.5 mL of 4% PFA into each well. After the brains were extracted, they were placed into these 4% PFA-filled wells and placed into the fridge for 4 - 8 hours. This step is done to fully fix the brain tissue. Afterwords, using a 1 mL transfer pipette, I switched out the 4% PFA and dumped it into the hazardous waste bucket in the fume hood. After emptying the well, I pipetted 1.5 mL of 30% sucrose into the brain-containing wells. The brains were placed back into the fridge. Sucrose is necessary prior to cryostat sectioning because it helps to prevent freeze damage of ice crystal formation, thus preserving cell formation at the time of sectioning.

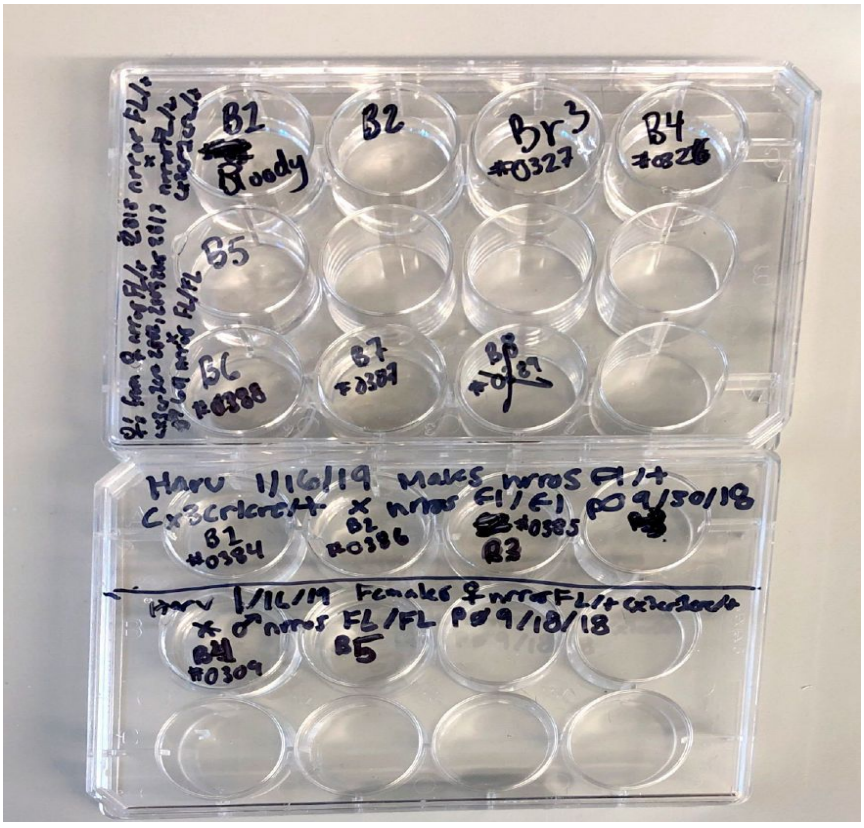

Figure 14: Labeled 12 well plates

Pictured here are the 12 well plates used for storing the brains in 4%PFA and subsequent 30% sucrose. The wells are labeled before perfusions are conducted. PFA and sucrose are added and removed from the wells via transfer pipette.

3.2.5. *Brain Embedding*

Once all the brains sunk to the bottom of the 30% sucrose-filled well (~ 1 day), they were transferred and embedded into optimal cutting temperature compound (OCT). This step is done to freeze the brains at -80 C. For cryostat tissue sectioning, brains must be frozen and encapsulated by OCT. First, cube plastic cartridges were ¾ filled with OCT. Next, the brains were scooped out from the wells via a modified 1 mL transfer pipette utensil and dried by covering them with kimwipes. Then, using tweezers, the brains were placed into the OCT-filled cartridges with a specific orientation. The brains needed to be positioned exactly in the center space of the cartridge, this is done to ease the set up of the cryostat. The cartridges are labeled with the brain number, genotype, P0 date, and perfusion date. Figure 15 shows the means required for OCT embedding.

Figure 15: OCT brain embedding

Pictured here are the tools needed to properly embed and freeze the brains in OCT. Brains are scooped out of the wells with the modified transfer pipette and dried off with kimwipes. Next, plastic cube cartridges are ¾ filled with OCT. The brains are placed into the middle of the OCT-filled cartridges. Cartridges are labeled and stored at 80 C.

3.2.6. *Brain Sectioning & Section Mounting*

Before I could perform antibody stainings to analyze the morphology and population of size of oligodendrocytes, microglia, and astrocytes, I needed to slice up the brain into thin coronal sections and mount them onto glass slides. Brains were sectioned in a rostral (front of the brain) to caudal (back of the brain) direction. Brain sectioning was done through two techniques: microtome and cryostat. Both methods require a paintbrush to carefully remove the section off a thin blade (after it has been sliced by the blade). Both methods also require the

brain to be frozen during sectioning. Both methods have their advantages and disadvantages. With the cryostat, sections can be mounted onto a glass slide right away, making it the faster technique for acquiring multiple small sections and arranging them on a single slide for subsequent comparative analysis. I also found sectioning with the cryostat to be more time-efficient than with the microtome because there is an extra step required before mounting with the microtome. After slicing the section and extracting it with the paint brush, the section was placed back into 30% sucrose-filled wells. Sections that have been microtomed were stained while inside the wells, and were mounted after stainings. Despite the lengthy process experienced with the microtomed sections, I found that unlike sections that have been cryostated, bubbles do not develop on the sections that have been microtomed. Another advantage I found with the microtome was that unlike the cryostat, multiple brains could be sectioned simultaneously via microtome.

Taking all these factors into account, the data coming from brains that were sectioned via cryostat was preferred because thinner section were yielded via cryostat, and thinner sections yielded higher immunostaining signal resolution. Microtome sections had a 40 micron thickness while cryostat sections had a 25 micron thickness. Initially, I tested out stainings on both microtome and cryostat sections. There was observable signals captured in both, however, cryostat sections had less background and higher resolution. Figure 16 shows both the microtome and cryostat apparatuses.

Figure 16: Cryostat and microtome instruments

The figure on the left is the cryostat apparatus and on the right is the microtome. Both use a thin blade to yield micron-thin brain section. Both techniques need a paintbrush to extract the sliced brain section off the blade. With the microtome, sections are placed into wells with 30% sucrose. Sections from the cryostat are immediately mounted onto a glass slide. Brains must be frozen in both methods. Cryostat produces thinner sections than the microtome. After initial staining, I preferred to section brains via cryostat because it provided higher signal resolution.

3.2.7. *Antibody Staining & Cover Slipping*

Immunohistochemical (IHC) staining uses antibodies to detect specific antigen markers on targeted cells inside fixed tissue mounted on a glass slide. IHC required a primary and secondary antibody staining on the brain sections. The

primary antibody is not labeled and has a high affinity for an epitope on a specific antigen. The antigens I needed to target were ones that are present in astrocytes, microglia, and oligodendrocytes. The secondary antibody is engineered to have a high binding affinity to the primary antibody. The secondary antibody has a fluorophore attached to it that emits a certain fluorescence under a particular wavelength. IHC stainings for oligodendrocytes, astrocytes, and microglia were conducted on fixed brain sections from CX3CR1cre/+ and NRROS FL/+ (heterozygous) mice and CX3CR1cre/+ and NRROS FL/FL (mutant) mice from the same litter and were of the same sex. Comparing sections of the same sex and same age, from the same litter minimizes unwanted variability in the data. Before staining the sections, I needed to first wash off remaining sucrose and follow that step up with blocking of nonspecific antibody binding sites.

Glass slides with brain sections fixed to them were labeled (P0 date, perfusion date, and genotype) and placed into a specialized plastic cup with chambers that held each slide in place. The slides were given three 5 minutes washes with 1X PBS. Next, the slides were removed and the side of the slide that did not have the mounted sections was dried with a kimwipe. I then placed the slides on a tray that held the slides flat, the side with the brain sections was facing me (seen in Figure 17). Wet paper towels were placed all around the inside edges of the tray to maintain a precipitated environment for the brain sections. Next, I used a hydrophobic pen and drew a barrier around the sections on the slide. This step was done so that all solutions, such as the blocking buffer and antibodies, that

were pipetted onto the flat surface of the slide with the fixed sections would not drip off the slides. Next, I pipetted 400 µL of 5% horse blocking serum (HBS) (see in appendix A.6) onto the sections and covered the tray. This step was done because before using specific antibodies to detect antigens, all potential nonspecific binding sites in the tissue sample must be blocked to prevent nonspecific antibody binding. If blocking is omitted or inadequate, the antibodies or other detection reagents may bind to a variety of sites that are not related to specific antibody–antigen reactivity. Antibodies can bind to many types of surfaces by simple adsorption, and they can bind to proteins because of charge-based, hydrophobic, and other types of interactions. HBS remained on the sections for 30 minutes.

Figure 17: Antibody staining set up

Shown in this image are the necessary tools and set up for primary and secondary antibody stainings of brain sections that have been mounted on glass slides.

Next, I removed the HBS and pipetted 350 µL of primary antibody onto the sections. I needed to make sure that all the brain sections were completely covered in the primary antibody solution. The primary antibody for oligodendrocytes was Olig2, for microglia/CNS macrophages it was Iba1, and for astrocytes it was GFAP. These primary antibodies bind to specific markers that are unique to each of these cell types, respectively. The protocols for making the primary antibody solution for oligodendrocytes, astrocytes, and CNS macrophages can be seen in appendix A.7. The tray was covered and the primary antibody solution remained on the brain sections for 4 hours at room temperature.

Next, the primary antibodies were removed from the slides and the sections were washed twice for 5 minutes with 1X PBS with 0.3% Triton and once with 1X PBS. Afterwords, the back of the slides were dried and then the 400 µL of secondary antibody solution was pipetted onto the sections (seen in appendix A.8). The species that the secondary antibody was raised in needed to be different from the species the primary antibody was raised in. This is because the secondary antibody should be against the host species of the primary antibody we are using in order to achieve secondary antibody binding. Secondary antibodies remained on the brain sections for 4 hours at room temperature. In order to prevent the likelihood of ambient light exciting the fluorophores bound to the secondary antibody, I covered the lid of the tray with aluminum foil. After removing the secondary antibodies, I placed the slides back into the plastic cup and washed the slides twice for 5 minutes in 1X PBS with 0.3% Triton.

Subsequent step was to pipette 200 µL of fluoromount onto the right side of the slides for coverslipping. After adding fluoromount to the slide, I covered the sections on the slide with a thin glass coverslip and let the fluoromount distribute evenly across the slide. Slides were then stored away for two days to allow for the brain sections to dry. Slides were placed inside a case to prevent light from exciting the fluorophore and dissipating its finite fluorescence activation.

3.2.8. *Axio Microscopy and Confocal Laser Microscopy*

After the slides dried, I took them to the microscope room and observed the stained brain sections under a fluorescent microscope. All the sections were co-stained, meaning that every section had the oligodendrocytes, astrocytes, and microglia cell stainings. However, under different wavelengths, 405nm, 488nm, and 549nm, I was able to isolate and individually inspect CNS macrophages/microglia, oligodendrocytes, and astrocytes, respectively. Before I could image the stained sections, I needed to choose which sections on the slides provided the best costaining of all three targeted cell types. I did not want to image sections on the slide that had unwanted fluorescence background and/or bubbles. Furthermore, in order to achieve the best possible comparative analysis between the heterozygous and mutant mice, I needed to pick a sections that were located in the same region of the brain in terms of rostral to caudal orientation. Choosing the best sections to image took some time, but once

they were chosen, I labeled them and booked the axio and confocal imaging microscopes located in second floor of Biomedical Sciences building.

I used the axio microscope to collect high resolution images of one hemisphere of both mutant and heterozygous brain sections. This was done in order to acquire a more comprehensive analysis of the stained glial cells. The confocal laser microscope was used to capture varied close up images of the brain sections. This was done in order to observe the cell morphology. Confocal imaging data was also used to quantify cell populations. Both the confocal and axio microscopes include software that automates the imaging process, which is imperative since the process involves the stitching of multiple captured images into one image. After, the images were transferred to my hard drive and downloaded onto my computer. Images were edited with Adobe Photoshop and organized with Adobe Illustrator.

4. Results

4.1. *Astrocyte immunostaining results & analysis*

GFAP was the antibody I used to target astrocytes in heterozygous and mutant brain sections. Glial fibrillary acidic protein (GFAP) is the hallmark intermediate filament protein in reactive astrocytes, and the GFAP antibody has a high binding affinity for this astrocyte-specific protein. It is good practice to compare similar brain sections. The stained brain sections that are compared and presented in Figure 18 came from two P115 mice from the same litter. Additionally, these two mice were females. One of these mice was a mutant, labeled with the NRROS FL/FL, CX3CR1cre/+ genotype, and the other was heterozygous, labeled with the NRROS FL/+, CX3CR1cre/+ genotype. Using axio microscopy and confocal laser microscopy, I was able to compare and contrast the morphology and population size of astrocytes in brain sections of both genotypes.

GFAP expression has been regarded as a sensitive and reliable marker that labels most, if not all, reactive astrocytes that are responding to CNS injuries. Another thing to note is that GFAP is not an absolute marker of all non-reactive astrocytes and is often not immunohistochemically detectable in astrocytes in healthy CNS tissue. Mature astrocytes in a healthy CNS do not express detectable

levels of GFAP and that GFAP expression by astrocytes exhibits both regional and local variability that is dynamically regulated by a large number of inter- and intra-cellular signaling molecules.

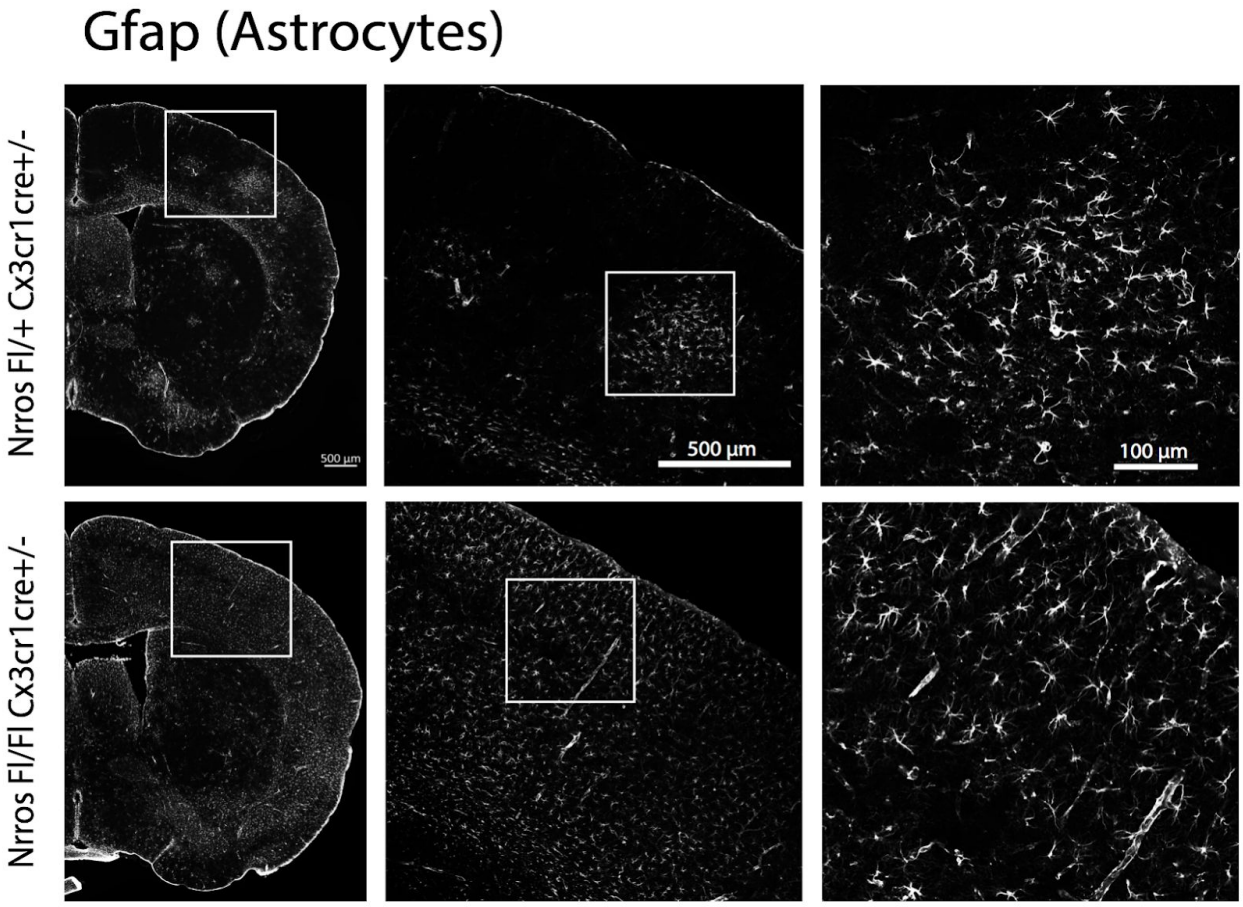

Figure 18: Reactive astrocyte levels in mutant and heterozygous CNS

Shown are the GFAP stainings of reactive astrocytes in mutant and heterozygous 115 day old adult brains. Both brains are from the same litter and are both extracted from females. Both seem to show similar astrocyte morphology. However, we can see different levels of astrogliosis between the heterozygous and mutant brain. Astrogliosis is an abnormal increase in the number of astrocytes due to the destruction of nearby neurons from CNS autoimmune responses, and/or

neurodegenerative disease. Looking at the cerebral cortex of the heterozygous staining, we can see that reactive astrocytes have a non-uniform distribution. While in the mutant brain, reactive astrocytes are uniformly present all over the cortex and the brain. The obvious difference in reactive astrocyte levels between the heterozygous and mutant brain, and the increased number of astrocytes in the mutant shows the importance of NRROS and how there is disease development taking place in its absence. Level of astrogliosis is lowered in the heterozygous brain, indicating that lower expression levels of NRROS provides an imperfect compensation mechanism. Nevertheless, the emergence of astrogliosis in the heterozygous brain shows that particularly normal expression levels of NRROS is vital for CNS homeostasis.

Analyzing the astrocytes stainings, we can see different levels of astrogliosis between the heterozygous and mutant brain. Looking at the cerebral cortex of the heterozygous staining, we can see that reactive astrocytes are present in non-uniform patches. In the mutant brain, reactive astrocytes are present uniformly throughout the cortex. The obvious difference in reactive astrocyte levels between the heterozygous and mutant brain, and the increased number of astrocytes in the mutant elucidates the importance of NRROS in disease development. The astrocyte staining data also shows that the partial reduction in NRROS expression (heterozygous) does not mirror the same magnitude of astrogliosis observed in the mutant (mutant). Instead, the level of astrogliosis is lowered in the heterozygous brain, indicating that lower expression levels of NRROS provides an imperfect compensation mechanism. Nevertheless, the

emergence of astrogliosis in the heterozygous brain shows that particularly normal expression levels of NRROS is vital for CNS homeostasis.

4.2. Oligodendrocyte immunostaining results & analysis

Using Olig2 antibody, I stained for oligodendrocytes because I wanted to further analyze our collaborators finding of normal presence of myelin sheath on axons. Oligodendrocytes function is to produce myelin sheath in the CNS.

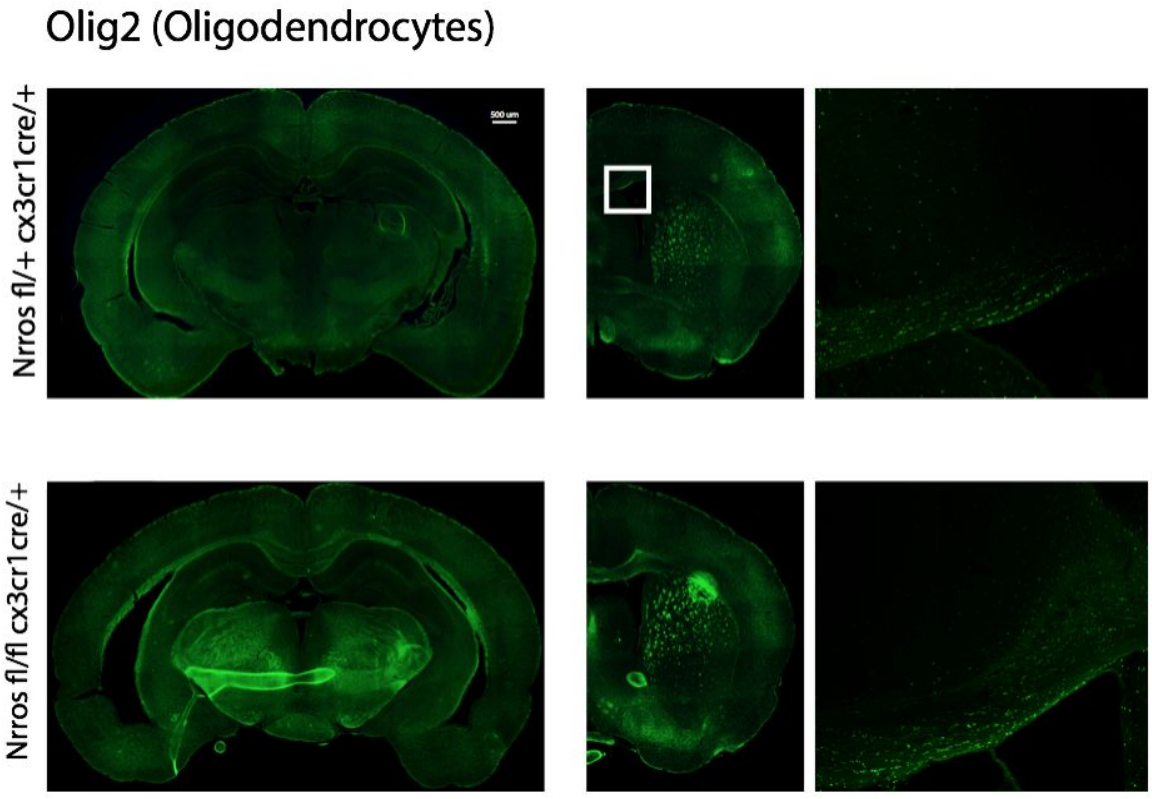

Figure 19: Oligodendrocyte levels in mutant and heterozygous CNS

Shown are the oligodendrocytes stainings, which were done with Olig2 antibody, of mutant and heterozygous adult brains. Oligodendrocytes produce myelin sheath in the CNS. Axio and

confocal imaging shows no substantial difference in the levels of oligodendrocytes between the two. This was expected since our collaborators found no disruption in myelin sheath generation in NRROS-deficient mice.

Staining the same brain sections used for the GFAP astrocyte staining and Iba1 macrophage staining, I was able to compare the presence of oligodendrocytes in the heterozygous and mutant brains. Looking at the Olig2 stained sections, I do not see a significant difference in the oligodendrocyte levels between the two brains. This was expected and more of a confirmation of our collaborators, since they found no disruption in myelin sheath generation in NRROS-deficient mice when looking at the sciatic nerve.

4.3. Microglia/CNS macrophage immunostaining results & analysis

Iba1 antibody was used to stain for Iba1 antigen markers, which are expressed by CNS macrophage cells, including microglia. The sections that were stained for Iba1 were from the same P115 brains that were used for the astrocyte and oligodendrocyte stainings, respectively. Looking at the Iba1 staining of the heterozygous and mutant brains (Figure 20), we can see a massive difference in the morphology of CNS macrophage cells.

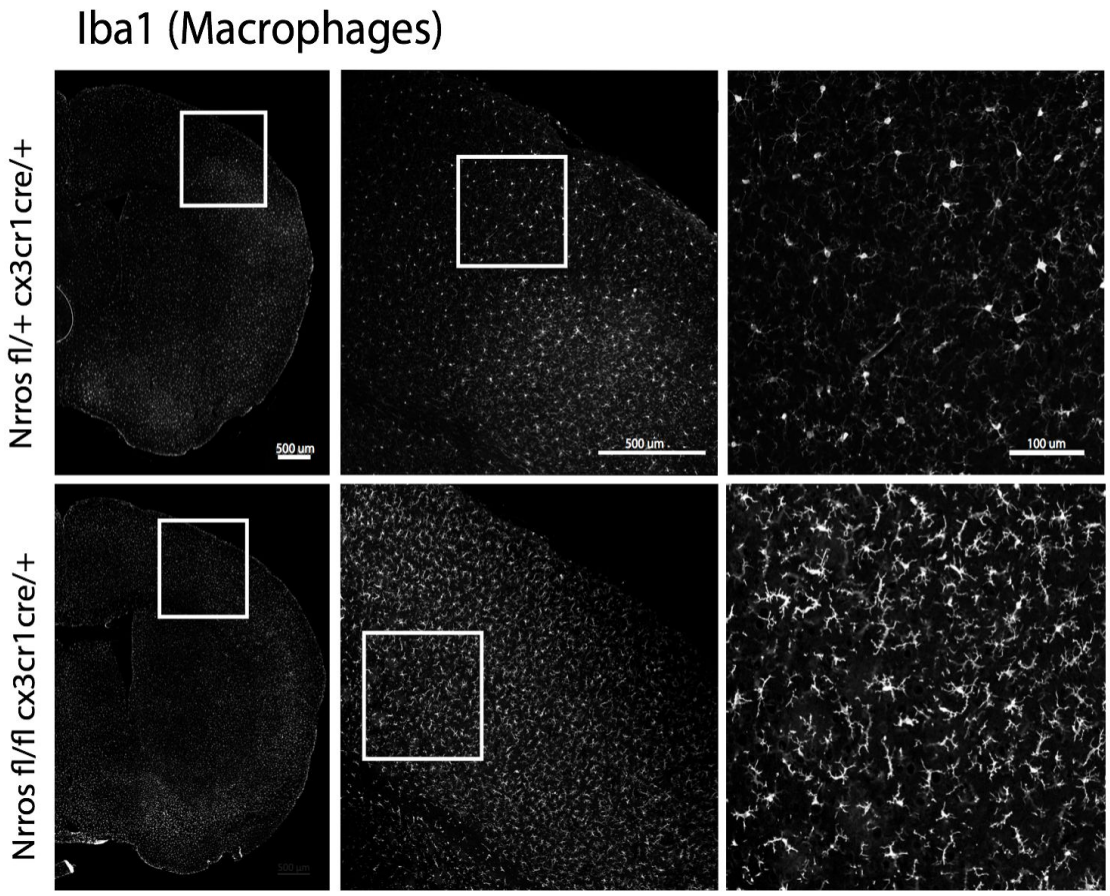

Figure 20: Macrophage morphology and population in mutant and heterozygous CNS

Iba1 stainings of the mutant and heterozygous brains detects the population and morphology of macrophage cells in the CNS, including microglia. The macrophage cells in mutant brain are uniformly activated all over brain, while a non uniform distribution of activated and steady-state microglia is exhibited in the heterozygous brain. The close up images are of the cerebral cortex, and they illustrate the morphological discrepancy between steady-state and activated microglia/macrophage cells. Small branching with a large circular cell body is described as a ramified state. Microglia display this morphology in a steady-state environment. Conversely, the microglia/macrophage cells exhibit a smaller rod-like cell body and substantially thicker branches in an activated state, which is a hallmark of neurological pathology.

In the heterozygous brain, we can see small branching from a large cell body, which is described as a ramified state. Microglia display this morphology in a steady-state environment. Conversely, the macrophage cells in the mutant brain exhibit a smaller rod-like cell body and substantially thicker branches. The rod-like morphology of the macrophages illustrated in the mutant Iba1 stainings is an evident characteristic in inflammatory responses. It is important to note that microglia activation, microgliosis, is a hallmark of brain pathology. Microglia morphology is modified into the observed rod-like structure in the process of responding to neuronal damage, and or removing the damaged cells. This further confirms that microglia activation does indeed induce the activation of reactive astrocytes.

Interestingly, the whole hemisphere of the heterozygous brain section is not uniformly populated with steady-state microglia cells. In fact, there are parts of the cerebral cortex that contains inflammatory microglia cells in an inflammatory state, similar to the microglia cells in the mutant. However, distinct from the fractional presence of activated microglia in the heterozygous brain, the mutant brain is fully covered by activated microglia/macrophage cells. This result further adds to the data seen in the heterozygous astrocyte stainings that the lower expression levels of NRROS still lead to the development of neurological pathology.

One thing to note here is that our collaborators recently examined the RNA-SEQ data of the microglia cells in the mutant brain. They describe these tissue-resident microglia in the mutant to be so transcriptionally different from normal microglia that these cells seem to be more transcriptionally related to perivascular macrophages, hence labeling them as *perivascular-like macrophages cells* (PLCs). I will be conducting another staining assay to check if the microglia cells observed in the mutant brain are actually not microglia cells, and instead PLCs. This data would solidify the developing theory that NRROS plays a critical role in the microglia developmental and migrational pathway.

5. Conclusion & Future Work

The objective of this project was to study the assortment of afflicted CNS cells in NRROS knockout mice. I bred and acquired the genotypes of homozygous NRROS knockout mice (mutants) and heterozygous NRROS knockout mice. I successfully perfused these mice at 5 months of age and extracted their brains while maintaining the integrity of their CNS cells. Obtaining and analyzing the neuroglial cells of 5 month old mice was favorable because the formation of deleterious phenotypes were fully manifested. Both microtome and cryostat instruments served to section the brains into thin slices, ranging from 25 μm to 50 μm. Using specific antibodies, I was able to carry out immunohistochemistry stainings that facilitated in analyzing the morphology and population of neuroglia cells and CNS macrophage cells.

The first few stainings were set up for oligodendrocyte and astrocyte analysis. These first stainings did not produce sufficient signals under the immunofluorescence microscope, restricting the detection of oligodendrocytes and astrocytes, alike. To deal with this roadblock, I adjusted the concentration of antibody-horse blocking solution and induced antigen retrieval on the brain sections prior to antibody stainings. Implementing antibody concentration adjustments and the addition of antigen retrieval to the staining protocol yielded discernible results.

Immunohistochemistry stainings of astrocyte cells in both heterozygous and mutant mice displayed phenotypes that are hallmarks of astrogliosis. However, the presence of astrogliosis was much higher in mutant mice in comparison to heterozygous mice. There was no prominent discrepancy in oligodendrocyte population between the het and mutant. In the mutant brain,

immune-activated CNS macrophages overwhelmed the brain parenchyma in comparison to the heterozygous brain. Additionally, TMEM119 stainings, a microglia-specific marker, confirmed that microglia cells were not detected in the mutant brain (data not imaged yet), supporting that the tissue-resident macrophage in NRROS-deficient is not microglia, but instead perivascular-like macrophage cells (PLCs). The loss of microglia and emergence of a transcriptionally distinct macrophage induces reactive astrocytes and initiates immune responses that are deleterious to the CNS. The research so far demonstrates the significance of NRROS in establishing CNS homeostasis and healthy brain function and its crucial role in microglia development and migration to the CNS.

Future work will be to conduct an assay that analyzes the neuromuscular junction at the hindlimb and the heart. This will be done to see if the cause of death in NRROS-deficient mice is due to the deterioration of axon branching in the muscles. I also plan to image my stainings for the TMEM119 data. This will be done to show that the macrophage present in the CNS tissue of NRROS-deficient mice is actually not microglia, but instead PLCs. Iba1 antibody stained for all all macrophages cell types in the CNS. I would like to isolate and focus on microglia population in future assays since microglia cells seem to be directly affected by the inability to express NRROS. I plan on using a cell quantification software to gather the cell count of the stained glial cell between the heterozygous and mutant brains. This will be done to see if there is a statistical difference in cell population size between the two genotypes. I also plan on conducting the same staining assays on WT mice to compare to the heterozygous staining data. Last, I plan on building an EKG with specific cutoff frequencies in order to record the heart contractions of these mice (both heterozygous and mutant) to see if they could be succumbing to cardiac arrest.

Bibliography

[1] Morgan, Deri, and Thomas E. DeCoursey. “Diversity of Voltage Gated Proton Channels.” *Frontiers in Bioscience: A Journal and Virtual Library* 8 (September 1, 2003): s1266-1279.

[2] Chung, Won-Suk, Christina A. Welsh, Ben A. Barres, and Beth Stevens. “Do Glia Drive Synaptic and Cognitive Impairment in Disease?” *Nature Neuroscience* 18, no. 11 (November 2015): 1539–45. https://doi.org/10.1038/nn.4142.

[3] Lobo, V., A. Patil, A. Phatak, and N. Chandra. “Free Radicals, Antioxidants and Functional Foods: Impact on Human Health.” *Pharmacognosy Reviews* 4, no. 8 (2010): 118–26. https://doi.org/10.4103/0973-7847.70902.

[4] Jäkel, Sarah, and Leda Dimou. “Glial Cells and Their Function in the Adult Brain: A Journey through the History of Their Ablation.” *Frontiers in Cellular Neuroscience* 11 (February 13, 2017). https://doi.org/10.3389/fncel.2017.00024.

[5] Harada, Kazuki, Taichi Kamiya, and Takashi Tsuboi. “Gliotransmitter Release from Astrocytes: Functional, Developmental and Pathological Implications in the Brain.” *Frontiers in Neuroscience* 9 (2016). https://doi.org/10.3389/fnins.2015.00499.

[6] Li, Qingyun, and Ben A. Barres. “Microglia and Macrophages in Brain Homeostasis and Disease.” *Nature Reviews Immunology* 18, no. 4 (April 2018): 225–42. https://doi.org/10.1038/nri.2017.125.

[7] Kierdorf, Katrin, Daniel Erny, Tobias Goldmann, Victor Sander, Christian Schulz, Elisa Gomez Perdiguero, Peter Wieghofer, et al. “Microglia Emerge from Erythromyeloid Precursors via Pu.1- and Irf8-Dependent Pathways.” *Nature Neuroscience* 16, no. 3 (March 2013): 273–80. https://doi.org/10.1038/nn.3318.

[8] Aguzzi, Adriano, Ben A. Barres, and Mariko L. Bennett. “Microglia: Scapegoat, Saboteur, or Something Else?” *Science (New York, N.Y.)* 339, no. 6116 (January 11, 2013): 156–61. https://doi.org/10.1126/science.1227901.

[9] Stein, Dirson J., Mailton F. Vasconcelos, Lucas Albrechet-Souza, Keila M. M. Ceresér, and Rosa M. M. de Almeida. “Microglial Over-Activation by Social Defeat Stress Contributes to Anxiety- and Depressive-Like Behaviors.” *Frontiers in Behavioral Neuroscience* 11 (2017). https://doi.org/10.3389/fnbeh.2017.00207.

[10] Herz, Jasmin, Anthony J. Filiano, Ashtyn Smith, Nir Yogev, and Jonathan Kipnis. “Myeloid Cells in the Central Nervous System.” *Immunity* 46, no. 6 (20 2017): 943–56. https://doi.org/10.1016/j.immuni.2017.06.007.

[11] Liddelow, Shane A., Kevin A. Guttenplan, Laura E. Clarke, Frederick C. Bennett, Christopher J. Bohlen, Lucas Schirmer, Mariko L. Bennett, et al. “Neurotoxic Reactive Astrocytes Are Induced by Activated Microglia.” *Nature* 541, no. 7638 (January 2017): 481–87. https://doi.org/10.1038/nature21029.

[12] Robinson, John M. “Reactive Oxygen Species in Phagocytic Leukocytes.” *Histochemistry and Cell Biology* 130, no. 2 (August 2008): 281–97. https://doi.org/10.1007/s00418-008-0461-4.

[13] Bonini, Marcelo G., and Asrar B. Malik. “Regulating the Regulator of ROS Production.” *Cell Research* 24, no. 8 (August 2014): 908–9. https://doi.org/10.1038/cr.2014.66.

[14] Nimmerjahn, Axel, Frank Kirchhoff, and Fritjof Helmchen. “Resting Microglial Cells Are Highly Dynamic Surveillants of Brain Parenchyma in Vivo.” *Science (New York, N.Y.)* 308, no. 5726 (May 27, 2005): 1314–18. https://doi.org/10.1126/science.1110647.

[15] Bedard, Karen, and Karl-Heinz Krause. "The NOX Family of ROS-Generating NADPH Oxidases: Physiology and Pathophysiology." *Physiological Reviews* 87, no. 1 (January 2007): 245–313. https://doi.org/10.1152/physrev.00044.2005.

[16] Levesque, Shannon, Thomas Taetzsch, Melinda E. Lull, Jo Anne Johnson, Constance McGraw, and Michelle L. Block. "The Role of MAC1 in Diesel Exhaust Particle-Induced Microglial Activation and Loss of Dopaminergic Neuron Function." *Journal of Neurochemistry* 125, no. 5 (June 2013): 756–65. https://doi.org/10.1111/jnc.12231.

[17] Noubade, Rajkumar, Kit Wong, Naruhisa Ota, Sascha Rutz, Celine Eidenschenk, Patricia A. Valdez, Jiabing Ding, et al. "NRROS Negatively Regulates Reactive Oxygen Species during Host Defence and Autoimmunity." *Nature* 509, no. 7499 (May 8, 2014): 235–39. https://doi.org/10.1038/nature13152.

[18] Rajkumar Noubade, Wong, Kit, Paolo Manzanillo, Naruhisa Ota, Oded Foreman, Jason A. Hackney, Brad A. Friedman, Rajita Pappu, Kimberly Scearce-Levie, and Wenjun Ouyang. "Mice Deficient in NRROS Show Abnormal Microglial Development and Neurological Disorders." *Nature Immunology* 18, no. 6 (2017): 633–41. https://doi.org/10.1038/ni.3743.

[19] Bradl, Monika, and Hans Lassmann. "Oligodendrocytes: Biology and Pathology." *Acta Neuropathologica* 119, no. 1 (January 2010): 37–53. https://doi.org/10.1007/s00401-009-0601-5.

[20] Parkitna, Jan Rodriguez, David Engblom, and Günther Schütz. "Generation of Cre Recombinase-Expressing Transgenic Mice Using Bacterial Artificial Chromosomes." *Methods in Molecular Biology (Clifton, N.J.)* 530 (2009): 325–42. https://doi.org/10.1007/978-1-59745-471-1_17.

[21] Wyss-Coray, Tony, and Joseph Rogers. "Inflammation in Alzheimer Disease-a Brief Review of the Basic Science and Clinical Literature." *Cold Spring Harbor Perspectives*

in Medicine 2, no. 1 (January 2012): a006346. https://doi.org/10.1101/cshperspect.a006346.

[22] André-Lévigne, Dominik, Ali Modarressi, Michael S. Pepper, and Brigitte Pittet-Cuénod. "Reactive Oxygen Species and NOX Enzymes Are Emerging as Key Players in Cutaneous Wound Repair." *International Journal of Molecular Sciences* 18, no. 10 (October 15, 2017). https://doi.org/10.3390/ijms18102149.

[23] K, Peter, and Technical Information Services. "Cre/Lox Breeding for Dummies." The Jackson Laboratory. Accessed February 3, 2019. https://www.jax.org/news-and-insights/jax-blog/

Appendix A

1. *2% Agarose Gel*
    - 160 mL of 1X TAE into 250 mL Erlenmeyer flask
    - Add 3 grams of agarose and mix
    - Microwave for ~3 minutes
    - Add 6 μL of ethidium bromide and mix
    - Pour onto gel box with well combs

2. *10 X PCR Buffer (50 mL)*
    - 10 mL of 1 M Tris, or tris(hydroxymethyl) aminomethane pH 8.4
    - 25 mL 1 M KCl
    - Add sterile H2O and volumize to 50 mL
    - Add those ingredients to 500 mL graduated cylinder
    - Filter with 25 mm filter paper and aliquot & label into 1.5 mL eppendorf tube

3. *1 X Tail Lysis Protocol (250 mL)*
    - Formulation: 100mM Tris HCl pH8.8, 5mM EDTA pH8.0, 0.2% SDS, 200mM NaCl

- Add the those ingredients to 200 mL nano-pure H2O in a 500 mL graduated cylinder.
- Allow reagents to mix on a stir plate for 5 minutes
- Bring final volume up to 250 mL using nano-pure H2O
- Aliquot & label into 50 mL conical tubes

4. 4% paraformaldehyde (PFA)

- Heat 650 mL nanopure H2O to ~ 65°C in 2L beaker with magnetic stir rod
- Add 32g of PFA to the heated nanopure H2O and turn on stir plate (inside hood)
- Add drops of 10N NaOH until solution clears and PFA is fully dissolved
- Allow to cool to room temperature (leave it stirring in the hood)
- Add 80 mL of 10X PBS
- Calibrate pH meter and use 3N HCl to get pH of solution down to 7.4 (exactly)
- Switch solution back to 1L graduated cylinder and volumize to 800mL with H2O
- Place back into 2L beaker in stir hood and get the pH back up to 7.4 with NaOH
- Filter solution with filter paper
- Aliquot & label into 50 mL conical tubes

5. 10X phosphate-buffered saline (PBS)

- Grab 4L beaker and fill up to 2L with nanopure H2O with magnetic stir rod
- Add 10.5g of NaH2PO4*H2O
- Add 92.8g of Na2HPO4*7H2O
- Add 360g of NaCl

- Place beaker on to stir plate in stir hood
- Stir until solution is completely clear
- Volumize to 4L with nanopure H2O
- Calibrate pH meter and make sure the pH is 7.3-7.4
- Filter and aliquot into 1L glass bottles and autoclave for 50’

6. 5% horse blocking serum with 0.3% Triton X-100 (HBS)
    - Add 2.5mL of horse serum into 50mL conical tube
    - Add 2.5mL of Triton X-100
    - Add 5mL of 10X PBS and shake
    - Volumize to 50mL with nanopure H2O
    - Store in the freezer
7. Primary antibody staining protocol (Did costaining on slides, so all mixed into one 1.5mL eppendorf tube before pipetting onto slides)
    7.1. Olig2 primary antibody staining (oligodendrocytes) for one mutant and one het slide
        - 1:500 concentration
        - Pipette 1mL of horse blocking serum into 1.5mL eppendorf tube
        - Add 2µL of Rat anti-Olig2 primary antibody
        - Pipette 500µL of solution onto each slide (cover sections fully)
    7.2. Iba1 primary antibody staining (CNS macrophages) for one mutant and one het slide
        - 1:400 concentration

- Pipette 1mL of horse blocking serum into 1.5mL eppendorf tube
- Add 2.5µL of Rabbit anti-Iba1 primary antibody
- Pipette 500µL of solution onto each slide (cover sections fully)

7.3. GFAP primary antibody staining (reactive astrocytes) for one mutant and one het slide

- 1:1000 concentration
- Pipette 1mL of horse blocking serum into 1.5mL eppendorf tube
- Add 1µL of Mouse anti-GFAP primary antibody
- Pipette 500µL of solution onto each slide (cover sections fully)

8. Secondary antibody staining protocol (Did costaining on slides, so all mixed into one 1.5mL eppendorf tube before pipetting onto slides)

8.1. Olig2 secondary antibody staining for one mutant and one het slide

- 1:500 concentration
- Pipette 1mL of horse blocking serum into 1.5mL eppendorf tube
- Add 2µL of Donkey anti-Rat 488nm secondary antibody
- Pipette 500µL of solution onto each slide (cover sections fully)

8.2. Iba1 secondary antibody staining for one mutant and one het slide

- 1:500 concentration
- Pipette 1mL of horse blocking serum into 1.5mL eppendorf tube
- Add 2µL of Donkey anti-Rabbit 405nm secondary antibody
- Pipette 500µL of solution onto each slide (cover sections fully)

8.3. GFAP secondary antibody staining for one mutant and one het slide

- 1:500 concentration
- Pipette 1mL of horse blocking serum into 1.5mL eppendorf tube
- Add 2µL of Donkey anti-Mouse 549nm secondary antibody
- Pipette 500µL of solution onto each slide (cover sections fully)

Appendix B

1. *Master Mix Protocol*

*All measurements are in microliters (µL)

Sample Count	10	15	20	25	30	35	40
10X PCR Buffer	23	34.5	46	57.5	69	80.5	92
MgCl2	11.5	17.25	23	28.75	34.5	40.25	46
dNTP	4.6	6.9	9.2	11.5	13.8	16.1	18.4
Primers	2	3	4	5	6	7	8
Taq Pol.	4.6	6.9	9.2	11.5	13.8	16.1	18.4
Nanopure H2O	152.3	228.45	304.6	380.75	456.9	533.05	609.2

2. *PCR Thermocycler Protocols*

2.1. NRROSFL/ PCR Program*

- WT Band = 429 - 454 bp
- Mutant Band = 552 - 600 bp
- Run for 34 - 35 cycles

Heating Lid Temp	94 °C	2:00
Denaturing Step	94 °C	0:40
Primer Annealing Temp	63-65 °C	1:00

Primer Extension Temp	72 °C	1:00
Final Extension Phase	72 °C	10:00
Optional Step	4 °C	5:00 or forever

2.2. CX3CR1cre/+ PCR Program

- WT Band = 302 bp
- Mutant Band = 380 bp
- Run for 34 - 35 cycles

Heating Lid Temp	94 °C	2:00
Denaturing Step	94 °C	0:40
Primer Annealing Temp	63-66 °C	1:00
Primer Extension Temp	72 °C	1:00
Final Extension Phase	72 °C	10:00
Optional Step	4 °C	5:00 or forever

2.3. Post-cre PCR Program

Internal Control Band (all mice have this band) = 250 - 280 bp

- Mutant Band = 489 bp
- Run for 34 - 35 cycles

Heating Lid Temp	94 °C	2:00
Denaturing Step	94 °C	0:40
Primer Annealing Temp	63-65 °C	1:00
Primer Extension Temp	72 °C	1:00

Final Extension Phase	72 °C	10:00
Optional Step	4 °C	5:00 or forever

2.4. Vavi-cre

- Internal Control Band (all vavicre mice have this band) = 260 - 282 bp
- Mutant Band = 394 - 438 bp
- Run for 35 cycles

Heating Lid Temp	94 °C	2:00
Denaturing Step	94 °C	0:40
Primer Annealing Temp	64-65 °C	1:00
Primer Extension Temp	72 °C	1:00
Final Extension Phase	72 °C	10:00
Optional Step	4 °C	5:00 or forever